Rethinking Plant-Based Materials Production:
Selective Growth of Tunable Materials Using Cell Culture Techniques

by
Ashley L. Beckwith

S.M. Mechanical Engineering, Massachusetts Institute of Technology 2018
B.S. Biomedical and Mechanical Engineering, Colorado State University 2015

Submitted to the Department of Mechanical Engineering
in Partial Fulfillment of the Requirements for the Degree of

Doctor of Philosophy

at the

MASSACHUSETTS INSTITUTE OF TECHNOLOGY

February 2022

Student Signature: _____
Department of Mechanical Engineering

Certified by: _____
Alan Grodzinsky, Committee Chair
Professor of Biological, Electrical, and Mechanical Engineering

Certified by: _____
Rohit Karnik, Committee Member
Professor of Mechanical Engineering
Associate Department Head for Education, Tata Professor

Certified by: _____
Luis Velásquez-García, Thesis Supervisor
Principal Research Scientist
Microsystems Technology Laboratories, MIT

Accepted by: _____
Nicolas Hadjiconstantinou
Chairman, Department Committee on Graduate Theses

Contents

1 Abstract

Each year, global forests shrink by billions of trees due to human activities and natural disasters. This sustained deforestation impacts both environment and economy. Forests are ecologically essential—supporting biodiversity, stabilizing ecosystems, and sequestering carbon. Trees also supply feedstock for building infrastructure, energy generation, production of consumer goods, textile manufacturing, and an increasing range of other economic activities. Biotechnology may hold the key to satisfying the growing demand for wood and wood-based products while staving off further deforestation and environmental disruption. This work explores the use of cell culture techniques to selectively generate plant-based materials without whole plant cultivation and harvest. The proposed approach allows for localized, high-density production, elimination of energy-intensive harvest and hauling, and reduced processing, while offering inherent climate resilience.

Employing a *Zinnia elegans* model system, this work provides the first proof-of-concept demonstrating net-shape, tunable plant material production *in vitro*. Central activities of the presented research include: (1) establishing knowledge to effectively direct cellular development, (2) devising and demonstrating mechanisms to direct material form, and (3) relating cellular-level properties to emergent material characteristics to allow tunable and predictable material outcomes.

First, using newly proposed metrics, cellular responses to applied culture conditions are quantified and mapped; selected environmental parameters including hormone concentration, medium pH, and cell density are shown to significantly influence cell differentiation and morphology.

Next, material form is directed through the casting and bioprinting of cell-laden hydrogel scaffolds. Gel-mediated culture enables plant material production both in forms and at scales that do not arise naturally in comparable whole plants. A maximum size for gel-based plant cultures has yet to be reached with prolonged cell viability maintained even at distances of more than 8.7 mm from the gel surface.

Finally, this work reports the first mechanical, physical, and microstructural characterization of 3-D printed, lab-grown plant materials and demonstrates material tunability with simple adjustments to culture conditions (e.g., hormone levels). Grown material properties vary significantly with hormone levels of the nutrient medium. The storage modulus of high-hormone samples presenting vascular cell types was elevated at 404.7 MPa $\pm$ 146.9 compared to low-hormone samples ($P = 0.033$) with storage modulus measuring at 135.3 $\pm$ 57.4 MPa. Hormone levels also impacted growth potential and physical material properties. High hormone samples saw only moderate increases in sample volume and mass (91% and 31%, respectively) compared with larger gains in low hormone formulations (398% and 119%, respectively), relative to a cell-free control. An examination of material microstructure reveals distinct cellular morphologies and identities for the evaluated growth conditions.

This work demonstrates the feasibility, tunability, and scaling potential of net-shape plant material cultivation—presenting new uses for plant culture technology, establishing novel methods for quantification of culture growth and development, and providing a first characterization of cultured plant materials. More importantly, this proof-of-concept illustrates the promise of a customizable, land-free approach to generating plant materials—a decisive first step towards the vision of tree-free wood products.

2 Acknowledgments

This work was made possible and sponsored in part by the Draper Scholars Program.

Thank you to my advisors, Luis Velásquez-García and Jeff Borenstein, for the trust and freedom to pursue an eccentric research proposition. I am grateful for the continued support and guidance in moving this project forward.

Thank you to my committee members: Professors Al Grodzinsky, Rohit Karnik, and Joel Voldman for your enthusiasm, advice, and patience as this project took shape with the help of your direction.

I am grateful to the four undergraduate researchers I have had the pleasure of working with: Maisha Prome, Andrea Garcia, Jordan Street, and Rachel Shen. Thank you for your insightful questions, diligent research, and your time. This project and I both benefited from the momentum and brainpower you brought to this effort.

Thank you to Erin Maryzek, Andy Dineen, and Henry Raczkowski of Draper for numerous consultations regarding and assistance with mechanical testing of materials. Thank you to Rick Crocker for help with lab setup and support. And thank you to the rest of the Draper staff for indulging my sometimes unorthodox methods.

I am appreciative of Professor Mary Gehring and Dr. Rebecca Povilus for early-stage plant-related research consultations.

Thank you to my lab-mates in the Velásquez Group for the continued support and feedback. Thank you especially to Anthony Taylor for putting up with the occasional office gnat infestation and ever-encroaching greenery.

Finally, thank you to my family and friends, who may not always know what I'm up to, but support me, nonetheless.

3 Introduction

Humans have long benefited from forestry resources. Trees serve as a stabilizing ecological influence—supporting a diverse body of living organisms, contributing to air and water flow and purification, sequestering carbon, and reinforcing local geology. The wood that trees provide continues to be an invaluable global resource for energy generation, infrastructure, and consumer goods [1]. The annual consumption of wood products is increasing with population growth and economic development [2] especially as industries seek alternatives to fossil-fuel derived products. With wood's widespread utility but naturally slow growth, modern cultivation models have not been able to sustainably support the growing demand. Crowther *et al.* report that deforestation, forest management, and land use change results in a net loss of 15.3 billion trees per year [3]. Evaluations by NASA showed that between 2000 and 2012, the world experienced a net loss of 1.5 million square kilometers of forests [4], amounting to an area larger than that of continental France, Germany, and Spain combined. At these rates of consumption, projections by Bologna *et al.* estimate that all of the world's forests could disappear within 100 – 200 years [5]. Meanwhile, the contributions of forests to an environmental equilibrium are needed now more than ever and as such, the preservation of forests is vital. A solution is urgently needed to address the ever-increasing demand for wood-based goods while alleviating the pressures placed on forests and arable lands. New cultivation approaches that improve yields, reduce waste, and minimize land usage are necessary to help rectify trends in deforestation and land conversion. In traditional whole plant systems, adjustments to production outputs face natural and narrow limitations. Instead, this thesis proposes a culture-based approach to material production which is not bound by the same constraints as whole plant cultivation strategies.

Despite widespread usage, whole trees generally make non-ideal feedstock with slow growth, low yields, and energy-intensive processing requirements. Trees can take decades to grow to a harvestable size. Low-value, fast-growing pulpwood trees typically require 10 to 20 years to achieve a profitable volume of timber [6]. Higher value saw timber takes

25 to 40 years to reach a harvestable size [7]. As a result of this slow growth, the impacts of poor forest management today can persist for generations. Unfortunately, the long-term incentives for good forestry practices are often at odds with near-term production demands. Best practices advise that one third of harvested tree material be left behind on the forest floor to regenerate the soil [7]. The maximum theoretical yield of tree material is therefore no more than two-thirds of the total cultivated plant matter. Of course, yields are further reduced by the varied utility of the remaining plant components. From the harvested crop, the top of the tree, bark, and small branches will commonly be discarded or burned, leaving much less than two thirds of the cultivated material to be used in the production of various wood-based infrastructure and consumer products. Exact yields will vary greatly depending on wood type and quality, as well as diameter and shape of the trunk. Beyond the intrinsic impracticalities resulting from natural tree form and growth characteristics, wood production faces the external challenges of susceptibility to pests, disease, and seasonal and climatic conditions all of which can further impact forestry yields and downstream production efforts. After harvest, the transport, refinement, and reconfiguration of wood materials require a significant investment of energy and financial capital (i.e., logging and transportation expenses make up a sizeable fraction of gate costs [8]). Because of inefficiencies in the cultivation and downstream processing of materials, work to generate and extract more value from harvested plants is continually ongoing.

Current approaches looking to address problems with tree yields and growth rates focus on modifications to whole plant growth characteristics. For example, using breeding and genetic modifications, tree plantation productivity has been improved to an extent by increasing growth rates and improving disease resistance[a] [1]. Active research is also using gene editing approaches to attempt to modify deposition rates and compositions of wood tissues with the hopes of improving yields and easing downstream processing requirements [2]. One common thread between nearly all efforts to improve wood production is their continued adherence to whole-organism agriculture—the implication being that these systems are fundamentally limited by the natural constraints allowing success-

[a]Traditionally, tree domestication involves selective breeding followed by clonal propagation [2]

ful growth and development of a complex living plant. Not only must modified organisms be capable of thriving, but they must also compete with and improve upon yields while sporting altered properties. In particular, when organismic benefits juxtapose economic benefits, the achievable range of genetic improvement may be quite narrow. For example, in pulping operations, certain polymers present in the plant cell walls (i.e., lignins) impede the isolation of high-purity cellulose and their presence necessitates multi-stage, energy-intensive processing as a result. Ideally, wood could be genetically modified to exhibit reduced lignin content and thus facilitate savings in downstream pulping operations. Lignin, however, plays an important role in growing plants and low-lignin mutants can be more susceptible to pests, disease, and slow growth [2]. Thus, realizing an "optimal" wood for pulping purposes could be so detrimental to growth rates that any advantage of the wood product is offset by reduced yields. Although economic productivity of whole tree cultivation has seen improvements as a result of breeding and genetic modification efforts over the years, the capacity for these techniques to address modern production challenges are limited. Ultimately, any sustainably grown whole-tree system will continue to output relatively low-yields of valuable products which will continue to require energy-intensive harvest, transport, and processing. Meanwhile, these systems continue to be susceptible to pests, diseases, natural disasters and climatic variability. Reduced genetic diversity that arises as a result of selective breeding and clonal propagation further weakens the genetic resilience of these remaining tree populations.

As an alternative solution to genetic modification of whole plants, this research effort propose using culture-based systems to selectively grow only the parts of the plants that are needed. As a result, theoretical yields approach one hundred percent of cultivated material and material properties can be manipulated without risk of impacting essential organism-level biological functions. With the direct growth of tunable plant materials in a controlled environment, climate is irrelevant and plant products can be grown locally, anywhere in the world. Most importantly, persistent inefficiencies in traditional practice could uniquely be addressed using the proposed production model.

This thesis proposes and explores the concept of *net-shape plant material cultivation*

through which desired tissues of plants are selectively grown in isolation, free from other plant components and produced in the exact geometries of interest. Culture-based generation of plant materials with tunable properties could minimize processing requirements and enable localized production of plant-based materials worldwide. The proposed approach makes use of a starter culture of cells that can be proliferated and sustained as a feedstock for prolonged periods. To initiate growth of tissue-like materials, starter cells are transferred to a nutrient-rich scaffold environment containing the necessary chemistry to induce differentiation into specialized cell types. The cell-laden growth scaffold is shaped using casting or bioprinting techniques to guide the growth of the final plant material.

The concept of cultured plant materials has not been well-explored to date [9, 10] and much work remains to be done to make this vision an implementable reality. This work takes the first steps toward the development of a practical approach for selective plant tissue generation and illustrates the feasibility and utility of such an approach through a proof-of-concept demonstration. With further development, a culture-based approach could offer numerous advantages over standard practice. The direct growth of materials: (i) does not require access to arable land and allows for compact production with potential for high yields per unit of land area, (ii) enables local, pesticide-free production with precise control over water usage reducing run-off and evaporation, (iii) allows continuous cultivation irrespective of season or climate, and (iv) facilitates growth of only desirable materials in convenient architectures thereby reducing waste, processing, and harvest cycle duration. Land-free production strategies have the potential to share in the fulfillment of biomass needs, reducing overall competition for arable and forested acreage and enabling increased preservation of natural lands in an effort crucial to the maintenance of the planet's biodiversity and capacity for carbon sequestration. Additionally, lab-based production can safely accommodate substantial application of genetic tools without fear of implications to the broader environment.

3.1 Prior Publication Notice

Some of the content included in this thesis has been previously published in a peer-reviewed journal (see Beckwith *et al.* [11]).

4 Background

4.1 Origins and State of Plant Cell Culture Methods

Plant cell culture emerged as a concept in 1902 with Gottlieb Haberland reportedly making the first attempt at isolating single cells from the leaves of a plant and maintaining them external to the organism [12]. Since that time, plant cell culture has become a sizable and growing industry [13]. Micropropagation, a process by which plant populations are cloned and rapidly multiplied by way of an intermediate cell culture step, is now a widely-used agricultural tool [13]. Micropropagation techniques are particularly useful for scaling the population of plants possessing desirable traits, or for rapidly bolstering populations of species which are endangered, slow to reproduce, or cannot be propagated by traditional methods (e.g., seeds, cuttings, division) [14, 15]. In addition to applications in amplifying plant populations, plant cell culture can also be used to produce a selection plant by-products. By the 1970's the capacity of culture systems to overcome traditional agricultural limitations and provide a local supply of valuable secondary metabolites was well-recognized [16]. Today, plant cell cultures produce a range of commercially-viable natural products and provides scalable propagation strategies for products of non-domesticated plants which are poorly suited to traditional agricultural cultivation [17]. Plant cells can even be designed to generate complex proteins with pharmaceutical value (e.g., Paclitaxel, berberines, rosmarinic acid, etc.) [17] that cannot otherwise be easily manufactured [18]. Protalix Biotherapeutics, Dow Agrosciences, Greenovation Biopharmaceuticals are among the suite of companies exploring the plant culture-derived pharmaceutical space. Protalix was the first to achieve FDA approval for plant cell-expressed acid β-glucosidase for treatment of Gaucher disease and has demonstrated systems for large-scale cultivation of plant cells and their by-products [19]. As technologies supporting scalable plant cell culture develop, high-value food and cosmetic ingredients (e.g., ginseng, atropine, alkaloids, nicotine, etc.) generated by cell culture have also found market footholds [17, 20]. Plant cultures are even being explored for the production of nanoparticles [21]. Despite the numerous applications of plant cell

culture that exist today, cell culture has apparently not yet been investigated as a means of producing plant materials [9]. As a result of the dearth of published information on the subject of cultured plant materials, this work pulls inspiration from a number of tangentially-related fields and applies this knowledge in a new space and to a new end.

Plants and plant products are of growing interest to the bioprinting community. Increasingly, plant products (e.g., cellulose, pectin) are employed as scaffold materials to support animal cell culture [22], but bioprinting of plant cells themselves has only been explored in a limited capacity to date [10]. Preliminary investigations into the field have focused on the development of suitable bioprinting strategies [23] and the application of immobilized cell culture techniques to investigate phenomena such as metabolite production [24] or single plant cell behavior in response to physical microenvironments [25]. Others have sought to employ gel-mediated culture of callus as a potential food production technique [26, 27]. These published efforts, promising steps into a young research space, are furthered by the detailed investigations of cell development and tissue-like generation included in this work. The demonstration of tunable biomaterial production as allowed by the characterization of controllable culture inputs marks significant progress towards the production of much-desired [25] *ex vivo* plant tissues. Together with the newly proposed applications for plant cell culture technologies, this work escalates explorations on plant cell bioprinting to high-impact, real-world solutions for biomass-driven industries.

4.2 Contextualizing Efforts in Selective Plant Material Growth

The discipline of 'tissue engineering' was first recognized in the 1980's, but the concept of isolated tissue generation or regeneration for wound healing efforts in mammals began even earlier. In some ways, mammalian tissue engineering efforts are analogous to this work as they similarly focus on generating an isolated tissue outside of the context of the whole organism. Because this type of tissue engineering in plant systems is relatively undeveloped, reviewing the historical trajectories of tissue engineering in animal systems

can help to predict the types and magnitudes of challenges likely to be faced in plant efforts.

Despite the vast existing body of knowledge on human physiology and development, access to large pools of research funds, and an ambitious flurry of excitement propelling efforts in animal tissue engineering, developments in the space have been slow. Tissue engineering is a complex, interdisciplinary field requiring an understanding the effects of numerous interactive factors on the growth and development of individual cells and tissues [28]. It can and does take many years of investigation to establish the resolution of knowledge required to elicit the desired coordination of cellular behavior. Both living components (i.e., cells) and their non-living surroundings (i.e., culture environment, scaffolding) contribute to the emergence of mimetic properties.

The first tissue-based regeneration therapies focused on skin [28]. The time from the conception of a skin substitute (1962) to the realization of a skin-like, living, two-layer composite (1981) stretched to roughly two decades. And although this skin-like material is among the closest researchers have come to recapitulating skin tissue *ex vivo* and serves a medical purpose even today [29], it still represents a poor model of the complex biological tissue it seeks to emulate [28].

Efforts to produce cardiac tissues *ex vivo* provide another interesting case study. In 1978, an attempt was made to repair a wounded heart by grafting cardiac tissue [30]. This early surgical effort launched the pursuit of a cardiac tissue substitute which could enable the repair and regeneration of injured heart tissue. By the early 2000's the field had moved away from *in vitro* tissue generation efforts and gravitated towards the implantation of biomimetic scaffolds seeded with undifferentiated pluripotent stem cell populations. This solution allowed for the development and specification of cells to be guided by the natural environment rather than requiring full suite of developmental triggers to be understood and controlled within the laboratory environment. Efforts to produce *ex vivo* cardiac tissue at medically-relevant scales proved difficult because of the need for vascularization and coordination of cellular alignment and function. By 2013, however, researchers had shown that cardiac tissue could be generated in a micro-

physiological format (small enough that vascularization was not needed) to be used in drug toxicity screening [31]. So, even 35 years after the conceptualization of local tissue replacement and regeneration, production of clinically-relevant lab-grown cardiac tissue remains a challenge.

The same strain of plant-focused tissue engineering is only just being investigated for the first time within this work. Given the comparative lack of species-specific knowledge and smaller scale of the existing research field and funding opportunities, many fundamental questions about plant tissue development are yet to be posed let alone answered. The field is still in its infancy, but there are reasons to be optimistic about a timeline to successful implementation. Compared to mammalian tissue engineering, plant systems offer the advantage that the final product does not need to achieve the same level of functionality. In mammalian tissue engineering, the intention is often to achieve long-term viability and successful integration within a living organism. In the case of plants, vascular plant tissues typically retain their utility long after death (and for human purposes, are typically only used long after death e.g., consider wood used in construction applications). In fact, even within living plants, the cells comprising some vascular tissues are "functionally dead" at maturity—one example being the xylem tissue which makes up wood. Therefore, the sustained viability and system integration required of mammalian systems is not required for plant material generation. Rather, the motivation of this research effort is to eventually recapitulate the structural utility of mature plant vascular tissue, but only maintain viability to the point of reaching this level of maturity and not beyond. This first foray into selective plant tissue production for the generation of plant materials aims to evaluate the feasibility of this effort and provide a vision for future work in this space.

4.3 Relevant Essentials of Plant Biology

The long-term vision of this thesis is to contribute to the net-shape production of tunable, wood-like materials *in vitro*. Wood consists of a vascular tissue known as

xylem—predominantly secondary xylem[b], which forms during later stages of plant growth and is responsible for water and solute transport throughout the plant [32]. Towards this end, this research aims to demonstrate the selective growth of plant materials which can be directed to express characteristics of the xylem.

Within a growing plant, xylem production begins with the division of cells of the cambium, a proliferative ring of tissue at the outer stem from which various vascular cell types develop [33]. The cells destined for xylem formation then undergo cellular expansion (enlargement and elongation) followed by cell wall thickening. This secondary cell wall (SCW) is deposited upon the completion of cellular growth and consists of a network of cellulose, hemicellulose, cell wall proteins, and eventually lignin. After the formation of the SCW, the cells undergo programmed cell death [32]. What remains is a functional corpse, with neighboring cells connecting to form a network of stiffened vessels to facilitate fluid transport [34]. The xylem comprises multiple cell types and the presence and prevalence of these cell types depend upon the plant species in question. Water-conducting cells of the xylem are collectively referred to as tracheary elements [34]. Tracheary elements are visually identifiable by their patterned, stiffened SCWs which enable the cells to retain their shape during water transport (Figure 1). While the primary cell wall is made up predominantly of non-cellulosic polysaccharides and some cellulose [35], the secondary cell wall (when present) contains a higher proportion of cellulose and also lignin in later stages of development [36].

For the purposes of this work, where the intention is to generate large quantities of specific plant tissues from a small starting quantity of plant matter, plant starter cells must be both proliferative and dexterous—capable of generating numerous daughter cells, and able to assume the desired cellular identity when prompted. Most living plant cells exhibit impressive developmental potency [37], i.e., they can give rise to plant cells of nearly any type or even an entire plant under the right environmental conditions [38]. Analogous to human stem cells, plant cells retain the ability to differentiate in response to local environmental cues [39]. Both their amenability to *in vitro* culti-

[b]Note that non-woody plants do not develop a secondary xylem, but will still possess xylem tissue

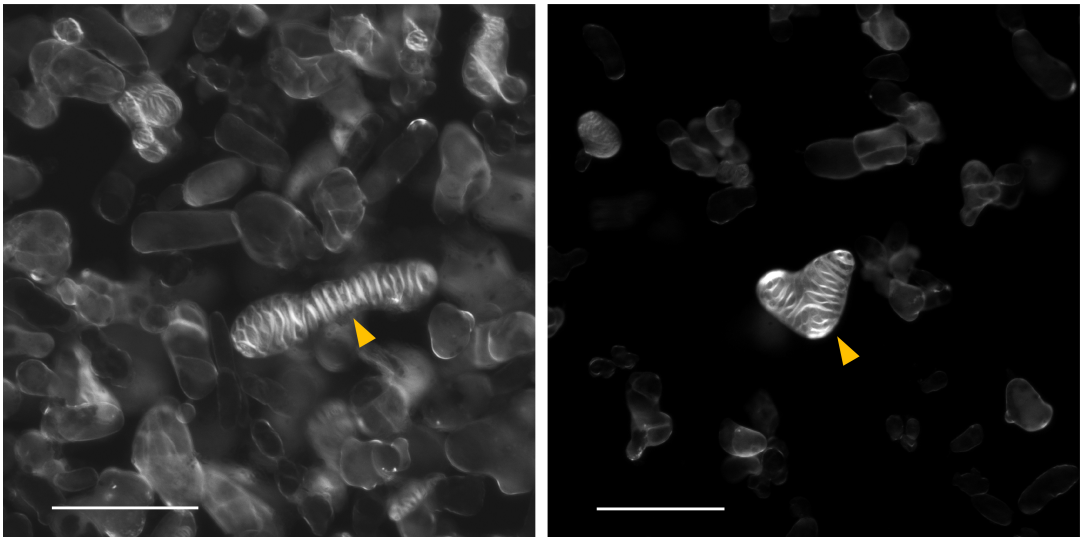

Figure 1: **Tracheary elements in *Z. elegans* suspension cultures visualized with Calcofluor White cell wall stain.** Tracheary elements can take on a variety of shapes, but characteristically present patterned secondary cell walls which fluoresce brightly compared to cells most other cell types that occur in culture. Orange arrows indicate examples of tracheary elements in a Zinnia suspension culture. Scale bars represent 100 micrometers.

vation and developmental dexterity make plant cells well-suited to externally directed growth. It has been shown that cultures of plant cells have great generative potential with doubling rates reported between 20 and 100 hours [40]. Some plant cultures can remain active and proliferative for extended timescales. Once established, plant cell cultures can be maintained for several years [39], established cell lines can also be frozen and preserved for later use [20]. The cues to stimulate differentiation of isolated plant cells into tracheary elements *in vitro* are better understood for some species than others. *Zinnia elegans* was selected for this proof-of-concept demonstration because the cues to trigger the differentiation of cells in culture are relatively well understood for this species. Specifically, simultaneous application of hormones from the auxin and cytokinin family can induce the transition of mesophyll cells isolated from Zinnia leaf samples into tracheary elements within a matter of days [41, 34].

In this proof-of-concept demonstration, net-shape materials are generated using cells sourced from the *Z. elegans* plant. *Z. elegans* is a practical model species for this demon-

stration because the plant is well-studied, grows rapidly, and wood-like vascular cells (tracheary elements) can be produced reliably in suspension cultures at frequencies greater than 60% [42, 41, 43]. Additionally, because Zinnia cells can be isolated readily through the maceration of leaves, cell cultures can be more rapidly established than species which require intermediate culture steps to generate a suspension of cells. With a model species like *Z. elegans*, feasibility of the proposed concept for plant material generation can be evaluated and processes developed which can later be adapted for higher-value, slower growing, and lesser-known species.

5 Research Framework

This research demonstrating the production of lab-grown, net-shape, and tunable plant materials consists of three core thrusts, summarized here:

1: Establishing and demonstrating knowledge to effectively direct cellular differentiation and morphological development. As in nature, cells are the building blocks of these lab-grown plant materials. In a whole organism, cellular-level features contribute to the ultimate properties of a specific plant tissue. It follows that, cell characteristics would be as important in determining the emergent properties of materials produced *in vitro*. The first section of this thesis focuses on developing an understanding of cellular response to easily controllable environmental parameters. The resulting knowledge enables thoughtful definition of culture parameters to guide the emergence of specific cellular morphologies and cell wall properties. Metrics characterizing cell viability, differentiation, and growth are first proposed for the quantification of culture behavior to allow for meaningful and measurable evaluations.

2: Developing and demonstrating mechanisms to direct material growth into specific forms. To improve on current practices and reduce processing required to isolate and re-shape natural materials, this work aims to grow materials in pre-defined shapes that represent near-final-form for the sample. Bioprinting and casting are used to define the cell-laden culture scaffolds and are shown to contain and direct growth of plant matter. Net-shape plant material cultivation offers the additional advantages of being able to produce plant materials in shapes and forms that are not naturally occurring.

3: Demonstrating opportunities for material-scale tunability through modulation of cellular growth. Understanding the relationship between cellular-level traits and emergent material characteristics is essential to producing materials with predictable and adjustable properties. Mechanical, physical, and microstructural attributes are assessed for material samples grown under different environmental conditions (and

thus exhibiting distinct cellular-level growth characteristics). This holistic assessment of materials from cellular to macroscopic scales provides a first look at the relationship between the two and facilitates the practical design of lab-grown, plant-based goods.

6 Quantifying Culture Development

Quantifiable metrics are critical to the progressive implementation of empirically-gathered knowledge. The following metrics, developed for this work, quantify collective culture development in a measurable way and allow for methodical selection of culture parameters to suit output requirements. The metrics are tabulated from micrographs and reflect live fraction, tracheary element differentiation (i.e., referred to as 'lignification' here), cell enlargement, and cell elongation in response to applied culture conditions.

6.1 Live Fraction

The live fraction metric is the ratio between the percentage of the micrograph occupied by cells marked with a viability probe (fluorescein diacetate (FDA), Millipore Sigma), A_L, and the percentage of the micrograph occupied by all cells marked with a cell wall stain (calcofluor white (CW), Millipore Sigma), A_T, i.e.,

$$LiveFraction\,[\%] = 100\% \times A_L/A_T \tag{1}$$

Live fraction provides insights into cell health and can act as a secondary indicator of tracheary element differentiation as cells undergo programmed cell death at late stages of development.

6.2 Lignification Metric

The lignification metric is the ratio between C_L, the number of tracheary elements in the micrograph exhibiting secondary cell wall patterning (Figure 1), and the corresponding A_T, i.e.,

$$Lignification\left[\%^{-1}\right] = C_L/A_T \tag{2}$$

Lignification metric quantifies the extent of culture differentiation into cells possessing a rigid, patterned cell wall characteristic of vascular cell types–the presence of which

may increase stiffness of the overall grown material. Cells are visually identified in micrographs by their unique cell wall patterning and counted manually to establish a C_L value for each image.

6.3 Enlargement Metric

The cell enlargement metric is the ratio between C_{en}–the number of cells in the micrograph with a maximum dimension greater than a certain threshold, and the corresponding A_T, i.e.,

$$Enlargement\left[\%^{-1}\right] = C_{en}/A_T \tag{3}$$

the threshold value for cell enlargement, l_α, represents the maximum dimension of cultured cells at 48 hours after cell isolation and is re-established for each experiment unless stated otherwise. Generally in these experiments, l_α is close to 84 μm for the extracted Zinnia mesophyll cells, but the exact value varies slightly with culture biology. The cell enlargement metric provides an indicator of average cell-level growth or swelling.

6.4 Elongation Metric

The cell elongation metric is the ratio between C_{el}–the number of cells in the micrograph with a maximum dimension greater than a certain threshold, and the corresponding A_T, i.e.,

$$Elongation\left[\%^{-1}\right] = C_{el}/A_T \tag{4}$$

the threshold value for cell elongation, l_β, represents the maximum dimension of cells grown in low-hormone media for 12 days that exhibit multi-directional enlargement without pronounced uniaxial elongation. The threshold value is re-established for each experiment unless stated otherwise. Generally, l_β is approximately equal to 119 mm, but the exact value can vary between experiments. Greater proportions of elongated cells may increase prevalence of cell-to-cell entanglement in confluent cultures, potentially

influencing grown material properties.

6.5 Data Collection Considerations

To collect imaging data, samples are marked with fluorescent probes, fluorescein diacetate (FDA) and calcofluor white (CW) as described in section 7.8. For determination of live cell area, A_L, and the total percent cell area, A_T, two-channel images visualizing FDA and CW were taken with focal plane adjusted to resolve FDA features. Lignified cell counts, enlargement, and elongation measurements were made on a corresponding single-channel CW image, with identical field of view but focus adjusted slightly to resolve CW features. In analyzing a sample at a given time point, all four metrics are obtained from the same set of micrographs.

7 Methods

7.1 *Z. elegans* Media Preparation

For the preparation of media, all listed ingredients (Table 1 or Table 2), except for BAP which is sensitive to autoclave sterilization, were combined in one liter of deionized water. The pH of the solution was adjusted to a value between 5.5 and 6.5 through the addition of sodium hydroxide and was subsequently autoclaved at 121°C for 20 minutes. The assigned, sterile quantity of BAP was added to the autoclaved medium in an aseptic environment. Sterile media may be stored at 4°C for up to 6 months[c].

Table 1: Recipe for *Z. elegans* Maintenance Medium (Ze-M)

Product Name	**Supplier**	**Quantity** [L^{-1} **water**]
N616 Nitsch Medium	Phytotech Labs	2.21g
Sucrose	Sigma Aldrich	10g
Mannitol	Sigma Aldrich	36.4g
α-Naphthaleneacetic acid (NAA)	Sigma Aldrich	0.001mg
6-Benzylaminopurine Solution (BAP)	Sigma Aldrich	1µl

Table 2: Recipe for *Z. elegans* Induction Medium (Ze-I) for Differentiation

Product Name	**Supplier**	**Quantity** [L^{-1} **water**]
N616 Nitsch Medium	Phytotech Labs	2.21g
Sucrose	Sigma Aldrich	10g
Mannitol	Sigma Aldrich	36.4g
α-Naphthaleneacetic acid	Sigma Aldrich	1mg
6-Benzylaminopurine Solution	Sigma Aldrich	1ml

In the case of gel media preparation, Gelzan CM (Sigma Aldrich) was added to the media solution[d] prior to autoclaving at concentrations between 3-5 g L^{-1}. To plate, the

[c]These are recommended storage times [44] for macro and micro salt solutions in regular use.

[d]Gellan gum is a commonly preferred gelling agent [44], [45] over agar and has been shown to yield improved growth in some cases [46]

liquefied gel media was mixed with the selected liquid medium at a ratio of 3:1 (v/v) while still warm.

The complete media formulation is provided in Table 3. The NAA stock solution was prepared as described by Mustafa *et al.* [44]. Note that plant hormones act at low concentrations [44]. Thus, preparation of an intermediate working solution is advised when recipes call for small total quantities of stock solutions (e.g., NAA and BAP additions in low-hormone (Ze-M) medium).

7.2 *Z. elegans* Cell Isolation

Inspired by methods of Fukuda and Komamine [41], *Z. elegans* cells were isolated by maceration of young zinnia leaves. The first true leaves collected from young zinnia plants were rinsed under running tap water for 5 minutes. Leaves were sterilized in a solution of 5 ml commercial bleach (Clorox), 95 ml of deionized water, and 200μl of Tween 20 (Sigma Aldrich) for 5 minutes. Subsequently, leaves were rinsed thoroughly with sterile distilled water to remove excess bleach and detergent. Rinsed leaves were sliced into strips, and gently ground between the surfaces of a small sieve and a stainless-steel spoon. The leaf matter was periodically rinsed with ZE-M media and, the rinsate, collected in a small bowl positioned beneath the supporting sieve. After completion of grinding, the process rinsate was collected and filtered through a 70 μm Cell Strainer (Fisher Scientific) to remove large debris. The filtered cell solution was centrifuged at 100 g for 8 minutes and resulting supernatant removed if more concentrated cell solutions were desired. In the described experiments, total volume at this stage was reduced to 10 ml, and a sample of the well-mixed, concentrated solution was combined with Evans Blue (Sigma-Aldrich) to be counted in a disposable hemocytometer. Once counted, fresh media was added to the cell suspension to achieve the desired concentration. Liquid cultures were then maintained at concentrations between 200,000 and 400,000 $cells \times ml^{-1}$ at 3 ml per well in a 6-well plate, wrapped in Parafilm. Cultures were maintained at 22°C in the dark on an orbital shaker operating at 80 rpm.

Table 3: Complete *Z. elegans* Media Formulations

Additive Name	**Ze-M Quantity** $[mg * L^{-1}]$	**Ze-I Quantity** $[mg * L^{-1}]$
Ammonium Nitrate	720	720
Boric Acid	10	10
Calcium Chloride, Anhydrous	166	166
Cupric Sulfate • $5H_2O$	0.025	0.025
Na_2 EDTA • $2H_2O$	37.26	37.26
Ferrous Sulfate • $7H_2O$	27.8	27.8
Magnesium Sulfate, Anhydrous	90.372	90.372
Manganese Sulfate • H_2O	18.9	18.9
Molybdic Acid (Sodium Salt) • $2H_2O$	0.25	0.25
Potassium Nitrate	950	950
Potassium Phosphate, Monobasic	68	68
Zinc Sulfate • $7H_2O$	10	10
D-Biotin	0.05	0.05
Folic Acid	0.5	0.5
Glycine (Free Base)	2	2
myo-Inositol	100	100
Nicotinic Acid (Free Acid)	5	5
Pyridoxine • HCl	0.5	0.5
Thiamine • HCl	0.5	0.5
Sucrose	10000	10000
Mannitol	36400	36400
α-Naphthaleneacetic acid	0.001	1
6-Benzylaminopurine Solution	0.001	1

7.3 *Z. elegans* Liquid and Gel Culture Preparations

Cells were incubated as prepared in the isolation procedure for 48 hours in low-hormone maintenance media (ZE-M) before transferring to any specialized experimental media. This incubation period improves differentiation rates when cells are later exposed to elevated levels of auxin and cytokinin. To replace media, cell solutions were centrifuged at 100 g for 8 minutes. The supernatant was removed and replaced with fresh medium.

To prepare gel cultures, cells were incubated in a low-hormone liquid medium for 48 hours as previously described. Just before plating, cultures were concentrated to four times the desired gel culture cell density. Freshly autoclaved and still liquid gel medium was mixed with liquid cell suspensions at a ratio of 3:1 (v/v). Once cooled to room temperature, cultures were sealed with parafilm and maintained in the dark at 22°C.

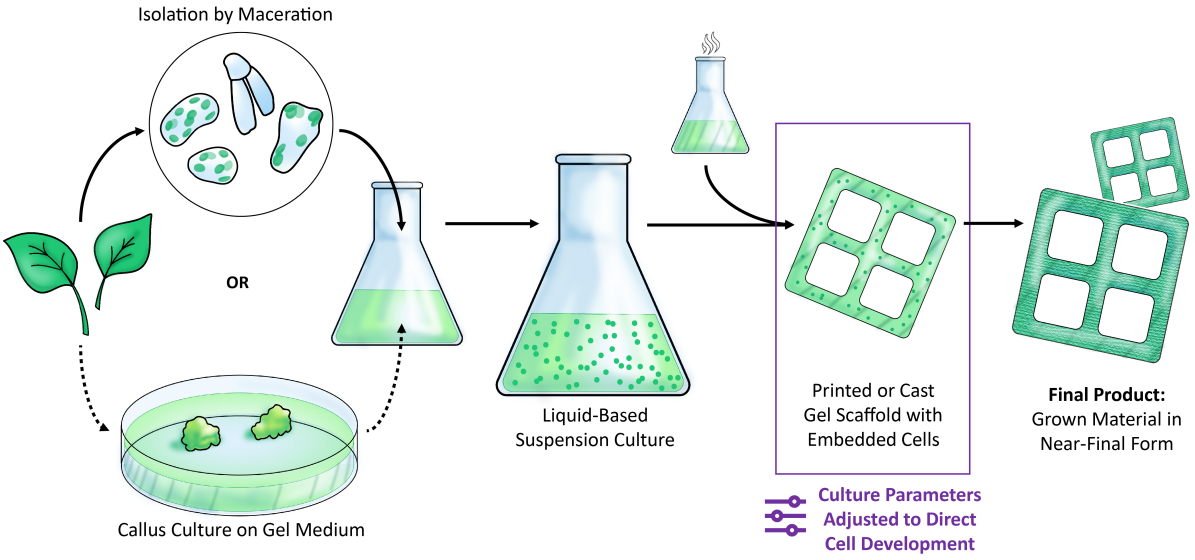

Figure 2: **Process flow of selective tissue-like growth from non-destructive plant sample.** From a small volume of plant material, *ex vivo* tissue-like constructs can be grown in the lab. The process of cell isolation from plant samples varies with plant species. In some species, like Zinnia, cells can be obtained directly through maceration of leaves. However, other species for which this approach may be adapted will require a callus culture to obtain friable cellular material. This adapted pathway is indicated by the dashed arrows. This figure was published in Beckwith *et al.* [11]

7.4 *Ex planta* Material Cultivation

From a small volume of plant material, cells were isolated to establish a liquid suspension culture. To initiate construct growth, concentrated cell suspension stock was mixed at a 1:3 ratio (v/v) with a thermosetting gel medium (containing Gelzan CM (Sigma Aldrich)). The resulting mixture was shaped prior to cooling by methods of casting or bioprinting. The process yields a culture of single cells dispersed within a gelled, shaped, nutrient-rich scaffold (Figure 2).

Early process steps are subject to variation depending on the plant species in use. For *Z. elegans*, cells were readily acquired through maceration of young leaves as described. Other plant species, including some woody species like *Pinus radiata*, will require an intermediate callus culture step, whereby an undifferentiated cell mass is initiated through prolonged culture atop a gelled, nutrient-rich medium [44] prior to the establishment of a liquid suspension culture. In both cases, collected cells are used to initiate a liquid culture where they may be cultivated, sub-cultured and utilized as a long-term feedstock for subsequent materials production.

7.5 Bioprinting Cell-Laden Structures

A mixture of liquefied gel media and concentrated cell solution were combined at a ratio of 3:1 (v/v) and loaded into a 10 ml syringe equipped with an 18-gage blunt-tipped needle. A Tissue Scribe bioprinter (3D Cultures, Philadelphia, Pennsylvania) deposited the gel solution into a petri dish in the programmed arrangements. During the printing process, the syringe temperature was maintained at 52°C to prevent solidification of the gel within the syringe. Printing Speed was maintained at 170 mm/min.

The printed, cell-laden scaffolds were sealed with parafilm and maintained in the dark at 22°C. After several days, a small amount of compatible liquid media was added to the petri dish to ensure that the samples did not dehydrate too quickly. Every 14 days, the petri dishes were briefly opened to allow for gas exchange and if the sample appeared dry (supplementary liquid has been taken up), an additional small volume of fresh liquid

medium was added to the petri dish to wet the sample.

7.6 Post-Cultivation Processing

Samples were rinsed twice with deionized water and then freed from the petri dish surface by completely submerging the sample in deionized water and nudging gently along its edges with a flat utensil. Using filter paper, samples were carefully transferred to and sandwiched between two flat surfaces covered with teflon sheets. Inverted petri dishes and covers were found to be useful for this purpose. Small filter paper strips were placed just in contact with the wet sample and extended to the edge of the drying fixture to facilitate dehydration. Assemblies were stored in a desiccator and allowed to dry.

7.7 Two-Channel Autofluorescence Imaging for Lignin Visualization

Autofluorescence of cell wall molecules allows for non-destructive visualization of cellular components. For lignin visualization samples were imaged on a Zeiss LSM 780 fluorescence microscope (Zeiss, Jena, Germany) at two excitation/emission pairs (355/488 nm and 455/535 nm). Taken individually, these excitation wavelengths can produce fluorescence in a range of natural fluorophores. Overlaying signals from both excitation/emission pairs, more specifically allows for lignin visualization as lignin more uniquely fluoresces at both settings [47].

7.8 Fluorescence Microscopy and Image Analysis

For liquid cultures, well-mixed 250 μl aliquots of cell suspension were transferred to 48 well plates for imaging. 20 $\mu l/ml$ fluorescein diacetate (FDA) stock solution (prepared at 2 mg/ml acetone) was added to the cell suspension and incubated in the dark for 20 minutes at room temperature. After the incubation period, 250 $\mu l/ml$ calcofluor white (CW) was added and the solution rested in the dark for another 5 minutes prior to imag-

ing. A Zeiss LSM780 confocal microscope was set to excitation/emission wavelengths of 265/440 nm (DAPI setting) for CW and 490/526 nm for FDA for imaging.

Gel cultures were also stained in two stages after wetting of the gel surface with a small amount of liquid medium otherwise matching the gel media formulation. Relative staining volumes were the same, but increased incubation times were required and vary with gel depth (e.g., incubation time requirements varied between 45 minutes and 2 hours).

Image analysis was performed using Image-J. Multi-channel images were first split into individual channels. Relevant cell areas were then selected through the thresholding function and measured. To ensure robustness of the analyzed data ranges, the images corresponding to the highest and lowest values of single sample are analyzed a total of 3 times, with the repeated results averaged to yield a final value for a given image.

For measurement of live area, A_L, and percent cell area, A_T, two-channel images including FDA and CW were taken with focal plane adjusted to resolve FDA features. Lignified cell counts, enlargement, and elongation measurements were made on a corresponding single-channel CW image, with identical field of view but focus adjusted slightly to resolve CW features.

7.9 Grown Material Sectioning and Imaging

Samples were embedded in paraffin wax and sliced into thin sections using a handheld microtome. Cross-sectional slices were transferred to a microscope slide and wetted with 10 μl of CW diluted in media (1:3 v/v). Samples were imaged on a Zeiss LSM 700 fluorescence microscope at 265/440 nm at a narrow range of focal planes. Between 1-8 images per sample were stacked using Adobe Photoshop 'Auto-blend' feature to produce composite images with improved clarity.

In cases where lignin visualization was also desirable, the processing was similar, but samples were additionally stained with Acriflavine stock solution (prepared at 1 mg/ml Acriflavine in water) diluted in water (6.2$\mu l/ml$ in water). 10$\mu l/ml$ of the imaging

solution was applied to samples following the application of CW. Samples were imaged immediately at $488/530nm$ to visualize lignin and processed as described.

7.10 Dynamic Mechanical Analysis (DMA)

DMA was chosen for mechanical analyses over more commonly known uniaxial tensile testing because DMA is both non-destructive and less sensitive to variations in sample geometry. Rectangular, bioprinted samples were prepared, cultivated and dehydrated for mechanical testing. Compared samples were generated on the same dates with the same cellular feedstock and grown for the same duration prior to dehydration. Time sweeps of applied, oscillating strains were imparted using a TA instruments Discovery Hybrid Rheometer-2 with the Film Tension Clamp fixture to ascertain elastic and viscous moduli values for dehydrated samples (Figure 3). Unless otherwise stated, time sweeps of applied, oscillating strains were imparted to ascertain modulus values for dehydrated samples. Tests were performed at an assigned strain amplitude (i.e., below the critical strain at 0.01%), a fixed frequency (0.1 Hz), and a constant temperature (20°C). Force, reported as stress, was measured in response to the applied strain and used to calculate the storage modulus (G') and loss modulus (G'') of the tested materials. Over the course of a DMA time sweep, samples were strained and relaxed multiple times, allowing for numerous replicate measurements to be taken on the same sample. With time, measurements stabilized. Sample-specific average measurements for G', G'', and $\tan\delta$ were obtained by averaging the values across the stable region; these individual sample averages were subsequently averaged across multiple samples, to obtain reported average values and standard deviations.

7.11 Physical Measurements

Length and width of rectangular samples were measured using calipers. Width was measured at three locations along the sample length and averaged. This was taken to be the absolute width of the sample for downstream calculations of sample volume. Sample

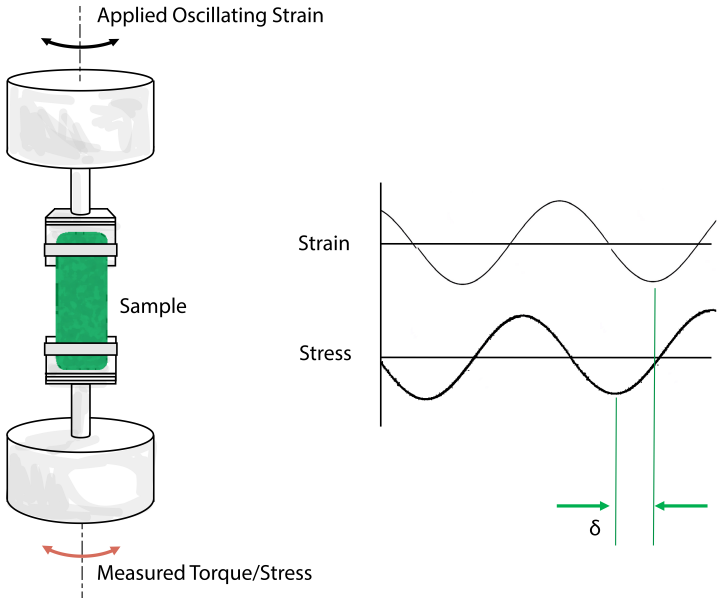

Figure 3: **DMA Setup.** A sample is fixed between two clamps. One clamp applies a defined oscillating strain to the sample while other fixture, remains stationary. Torque or stress data is collected at the stationary clamp. The relationship between applied strain and resulting stress provides insights on mechanical properties of the sample. The phase shift between the stress and strain data is known as δ.

thickness was measured using a benchtop micrometer. Again, samples were measured at three locations along the sample length and averaged. This was taken to be the absolute sample thickness for downstream calculations of sample volume. Sample density was obtained by dividing sample mass, determined with a mass balance, by calculated sample volume. For the purposes of the enclosed analyses, where the priority is understanding growth trends rather than absolute mechanical properties, the density measurement of a given sample was assumed to be exact (with an error of zero) for ease of standard deviation reporting. For a particular treatment group, these masses or densities are presented as averaged values across measured samples with sample standard deviations reflecting the variance among the "exact" sample-specific values.

7.12 Statistical Methods

7.12.1 Statistical Methods for Image Analysis

Unless otherwise specified, data reported for a specific timepoint and treatment were averaged across all images evaluated for that treatment on that day. Error bars on provided data plots represent one sample standard deviation above and below the mean. Two sample t-tests were performed at a confidence level of 95 percent to establish P-values between pairs of datasets (Matlab). In the case of hormone response experiments, in which cell response to two factors were investigated simultaneously, a full factorial design was performed at 4, near-equally-incremented levels of each hormone concentration (i.e. amounting to 16 individual hormone combinations). Factorial approaches are generally preferred to one-factor-at-a-time experimentation because they enable the detection of interaction effects between variables. The resulting response metrics were mapped using the Matlab contour function.

7.12.2 Statistical Methods for Mechanical Analysis

Over the course of a DMA time sweep, samples were strained and relaxed multiple times, allowing for numerous replicate measurements to be taken on the same sample. With time, measurements stabilized. Sample-specific average measurements for G', G'', and $\tan(\delta)$ were obtained by averaging the values across this stable region. These individual sample averages were subsequently averaged across multiple samples, to obtain reported average values and standard deviations.

8 Tuning Cell Development

A wide range of chemical and environmental factors play a role in governing plant cell development. For the purpose of reliably directing cell growth in a culture setting, three influential and independently controllable parameters were selected for analysis: the interactive effect of two hormone concentrations, the medium pH, and the initial cell density. Cell response to variation in these parameters was mapped using the four proposed metrics: live fraction, lignification, enlargement and elongation.

Although hormone concentration [41, 48] , pH [49], cell density [34] and other factors [50, 51] have been independently investigated to various extents, thorough re-evaluation of these variables is required in order to: (a) verify relevant cell behavior in spite of new, simplified media recipes (Tables 1 and 2), (b) characterize previously unreported developmental traits such as enlargement and elongation in tandem, (c) demonstrate the utility of new metrics to quantify cell development, and (d) contribute to the limited information available on cell growth and development in dispersed gel culture.

8.1 Effects of Hormone Concentrations on Cell Development

Two hormone classes, i.e., auxin and cytokinin, are drivers of plant cell development [38] and are critical to vascular tissue development in particular [43]. Both auxin and cytokinin independently control a wide range of cell behaviors [52]. Considered together, the hormones elicit complex, interactive effects. For example, elevated levels of both auxin and cytokinin can induce the differentiation of *Z. elegans* cells into lignified tracheary elements [53], while collectively low hormone concentrations are provided to *Z. elegans* cultures to encourage maintenance and proliferation without further differentiation. Cell morphology and development at unbalanced ratios of auxin and cytokinin concentrations have not been as well-characterized, particularly in relation to cell enlargement and elongation.

A full factorial experiment was performed to evaluate cellular development at a range of hormone concentrations over a 12-day culture period, using the previously described

metrics. After a 48 hour acclimation phase in which isolated cells were cultured in low-hormone media, samples were transferred to treatment media and imaged periodically over the course of the subsequent 10 days. The two hormones selected for evaluation are commonly employed in plant cell culture: a synthetic auxin— α-naphthaleneacetic acid (NAA), and a synthetic cytokinin— 6-benzylaminopurine solution (BAP). Hormone concentrations ranged from 0.001 mg/ml, as recommended for culture maintenance, to 1.5 mg/ml —one and a half times the concentration regularly cited for tracheary element induction [42], evaluated at approximately 0.5 mg/ml intervals. Contour plots of live fraction, lignification, enlargement, and elongation metrics map the cellular responses to the varied hormone levels (Figure 4). The experimental results demonstrate that tuning hormone concentrations allows for control over final cellular composition of the treated culture.

8.1.1 Discussion of Initial Factorial Results

In low-hormone (Ze-M) maintenance media, cells exhibit high levels of viability ($> 70\%$ live fraction) after ten days and the corresponding level of lignification remains at or near zero. Cells in low-hormone treatment media tend to enlarge over time, but experience limited uniaxial elongation. Lignification levels were elevated in the regions where both NAA and BAP ranged between 0.5 mg/ml and 1 mg/ml with a cumulative lignification maxima at NAA at 0.5 mg/ml (500 $\mu l/L$ of stock solution) and BAP at 1 mg/ml (1000 $\mu l/L$ of stock solution); correspondingly, these hormone levels exhibit the lowest live fraction at day 12—a reasonable result as lignifying tracheary elements undergo programmed cell death in the final stages of differentiation [32]. An increasing lignification metric could thus sensibly correspond to a declining live fraction. At the final time point, cumulative lignification values (Figure 4b) and daily lignification values (Figure 5) show indications of this inverse trend with live fraction, although the correlation is not exact.

Results also indicate that with the selected base media formulation, BAP plays an important role in determining the elongation fate of cells, although this control is commonly attributed to auxin specifically [42, 51, 52]. Elongation metric plotted across

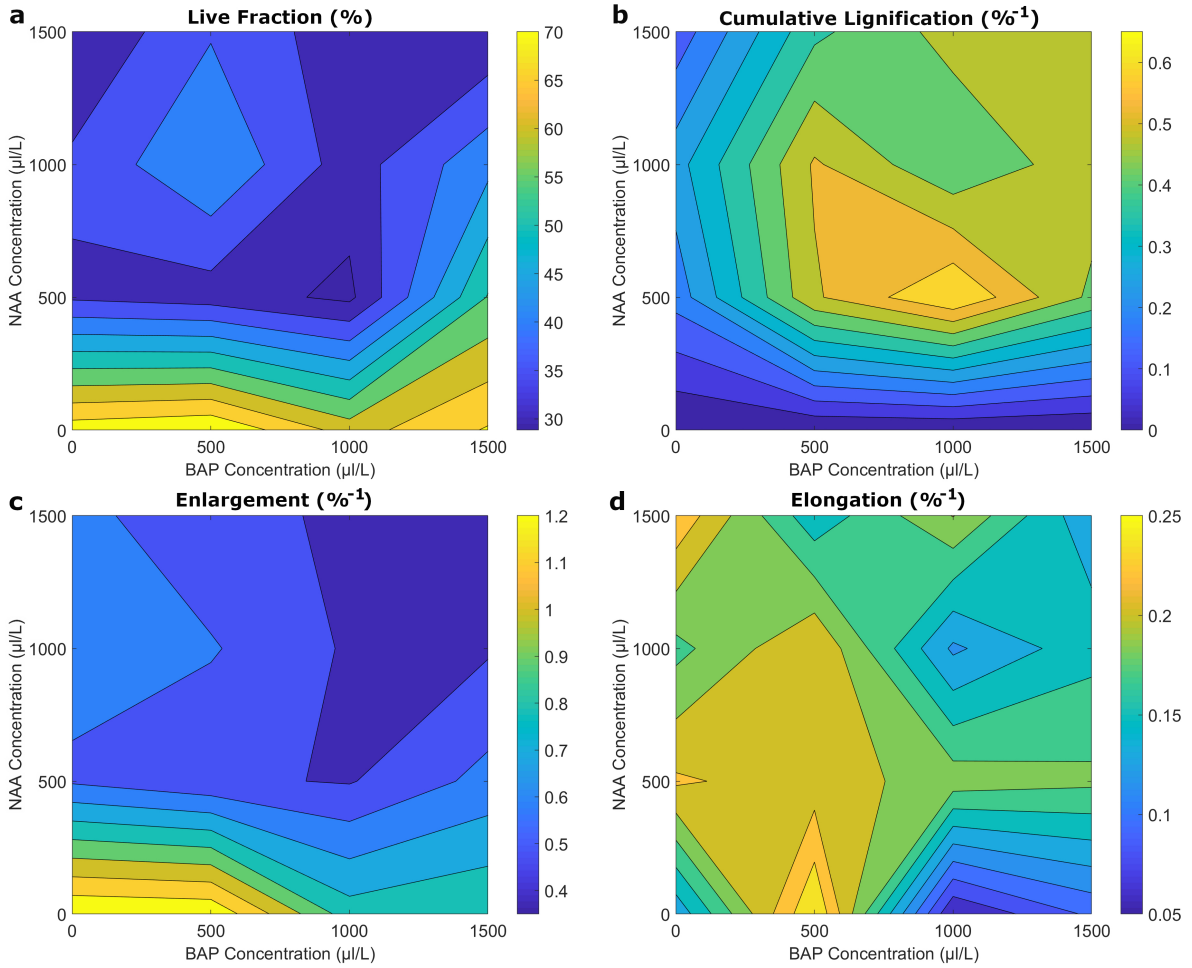

Figure 4: **Characterization of cell response to varied hormone levels.** Live fraction (a), cumulative lignification metric (b), enlargement metric (c), and elongation metric (d) on the twelfth day in culture are mapped for cells exposed to varied levels of NAA and BAP. N = 4 - 5 images per datum point. For (a), (b), (c), and (d), the average standard deviations for analyzed data points across each map are 6.63, 0.034, 0.095, and 0.055, respectively. This figure was published in Beckwith *et al.* [11].

hormone levels shows that when BAP is elevated beyond 1000 $\mu l/L$, elongation tends to be reduced across most NAA concentrations (Figure 4d).

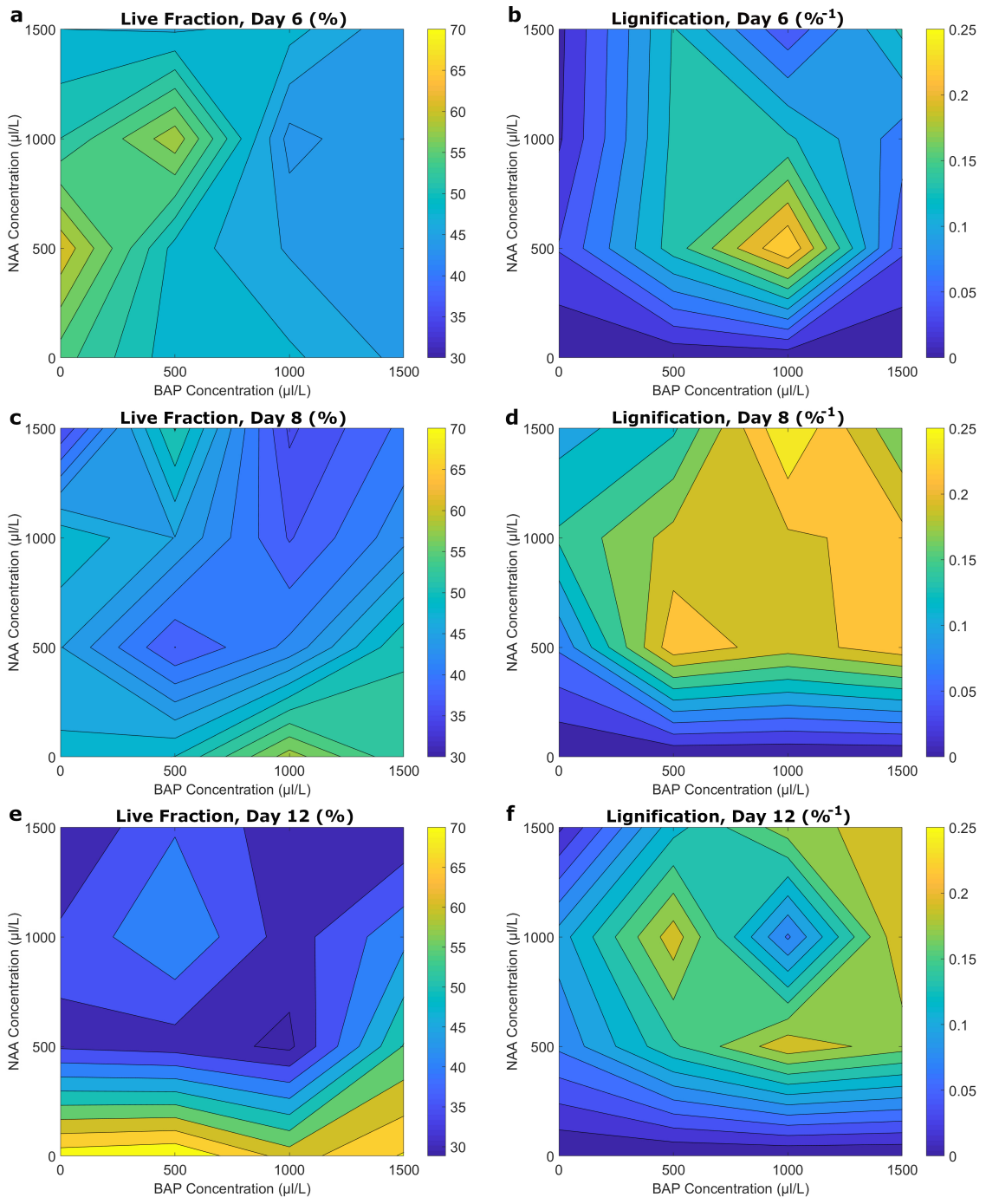

Figure 5: **Day-by-day comparison of live fraction and daily lignification metrics at varied hormone levels.** Day-by-day comparisons of live fraction (left column) and daily lignification metric (right column) for days 6 (a), (b), 8 (c), (d), and 12 (e), (f) of *Z. elegans* cultures illustrate that the two metrics are somewhat inversely related. N = 4 - 5 images per datum point. For (a), (b), (c), (d), (e), and (f) the average standard deviations of analyzed data points across the contour plots are 4.5, 0.028, 5.25, 0.052, 6.63, and 0.034, respectively. This figure was published in Beckwith *et al.* [11].

8.2 Factorial Experiment Verification

A follow-up experiment was performed to evaluate the repeatability of the DOE results with a new biological starter (i.e., a new batch of extracted cells). The verification experiment included replicate tests of previously evaluated hormone combinations as well as previously untested intermediate combinations (Figure 6). The experiment was performed and analyzed as in the initial factorial experiment. Verification data was compared against initial data for repeated test points or linearly interpolated predicted values for the previously-untested, intermediate hormone combinations (Table 4).

8.2.1 Discussion of Verification Results

Cellular behavior, as quantified by the four established metrics reflected the same patterns seen in the initial factorial experiment. Live fraction was elevated in low-hormone cultures, reaching values nearing 80%. Meanwhile, viability declined in cultures undergoing high rates of differentiation into tracheary elements. The inversion between live fraction and lignification metrics is evident in Figure 7 and is consistent with trends witnessed in the original tests. Treatments 2 and 3 yielded the highest magnitude cumulative and daily lignification metrics (Figures 7 and 8) and these formulations with media 6 and 7 span the region of maximal differentiation seen previously. Trends in

Table 4: **Treatment group and corresponding hormone levels. Asterisks indicate repeated test points tested in original factorial experiment; the remaining samples represent intermediate values not previously tested.**

Treatment ID	**BAP Concentration** ($\mu l/L$)	**NAA Concentration** ($\mu l/L$)
1*	1	1
2*	1000	500
3*	1000	1000
4	250	250
5	1250	250
6	750	750
7	250	1250

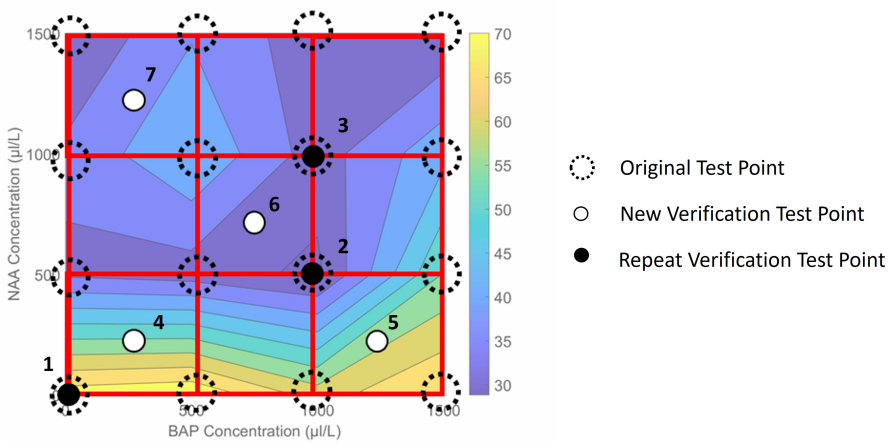

Figure 6: **Graphical representation of test points for verification experiments overlaid on original DOE contour plot for comparison.** Dashed circles represent original test points, solid black circles represent repeated test points and solid white circles represent intermediate, previously untested points. Numbers correspond to Treatment ID's with NAA/BAP hormone levels listed in Table 4.

live fraction and lignification thus appear to exhibit good consistency even across unique Zinnia samples.

As in the factorial experiments, enlargement metric was highest for low-hormone media formulations. Interestingly, elongation tended to be pronounced in samples with lower levels of tracheary element differentiation. (See Figure 9). This could be a result of the early commitment of differentiating cells to their developmental pathway which involves early secondary cell wall deposition and the cessation of further growth. By comparison, elongation tends to become evident in more mature cultures. Thus, high differentiation rates would lead to a smaller pool of remaining cells with the potential for elongation. In the pursuit of more naturally-representative materials, the delay of differentiation into vascular cell types until after the cells have elongated may be preferable.

8.2.2 Comparison to Original Model

In these verification samples, relative trends in cell development have remained consistent with original data. A look at absolute comparisons between the developed model and verification results provides additional insights–elucidating other key considerations

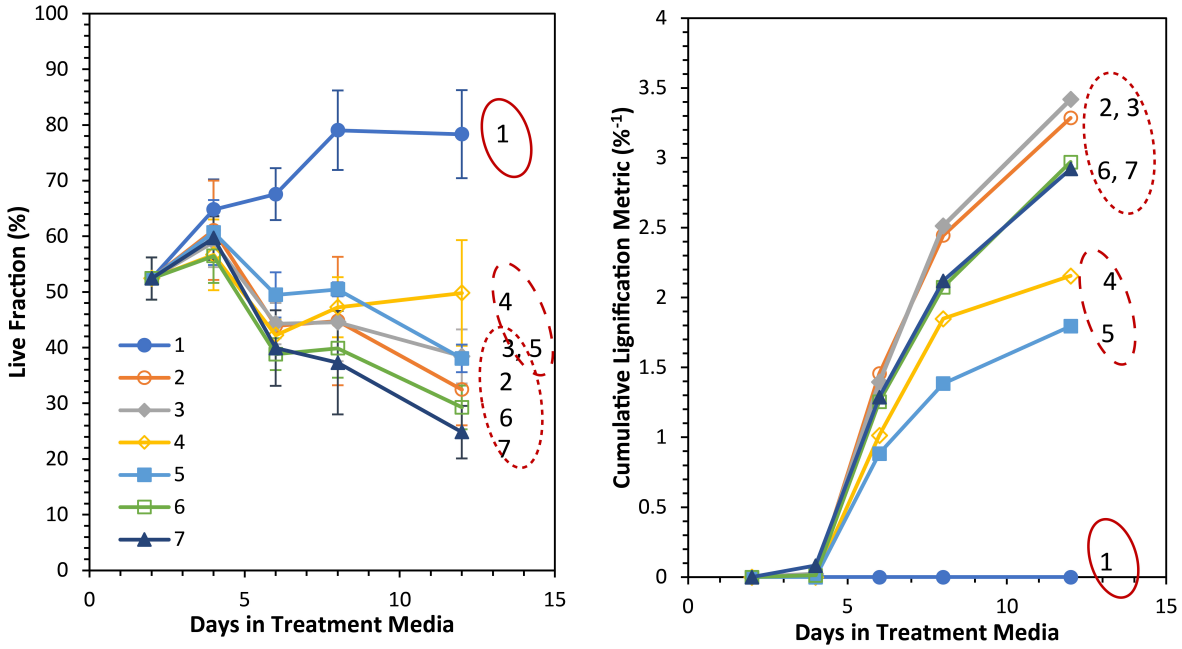

Figure 7: **Live fraction (a) and cumulative lignification metric (b) versus time for the cultures grown in media defined in Table 4.** As reported previously, live fraction tends to trend inversely with lignification as shown by the inversion of groupings highlighted with dashed, red ellipses. The 1 to 7 labels of the curves correspond to the treatments listed on Table 1. N = 6 images per datum point.

which could contribute to improved culture tunability.

Despite differences in the initial live fraction, the metrics for original and verification cultures tended to converge to comparable values by the later stages of growth. For repeated experimental conditions (i.e., media 1, 2, 3), daily live fraction is plotted for both the original and verification experiments (Figure 10) and correlations are evident. For new verification test conditions (i.e., intermediate hormone conditions 4, 5, 6, 7), daily live fraction is compared against predicted values obtained by linearly interpolating the midpoint values from original DOE data (Figure 11). Again, the predicted values correspond well to the verification data in most cases. The deviation from predicted values seen for media 5, may be result from non-linearity of cellular response, and thus prediction inaccuracy, in this region where change in original DOE live fraction is dramatic across the sector.

For lignification metrics, although trends in differentiation behavior remained con-

sistent (i.e, media 2 and 3 exhibiting highest levels of lignification for the tested media selections, and media 1 the lowest), the magnitude of cumulative lignification was elevated in verification tests compared to original data (Figure 12). This shift in absolute value is likely attributable to: (1) the increased live fraction seen in verification samples prior to the differentiation (i.e., thus, more viable cells capable of differentiating and a higher effective cell density which has been shown to improve differentiation rates), as well as (2) natural biological variation of Zinnia plant sources. Most importantly, patterns of behavior remain consistent in spite of the variability of biological source samples.

As with the other metrics, trends in cellular enlargement and elongation were consistent in relative terms to the original data. However, in the verification test, both enlargement and elongation metrics were reduced compared to the original results (Figure 13)–contrasting with the increases seen in lignification. This aligns with the predicted interplay between the rapid commitment and differentiation into tracheary elements and the slower expansion and elongation processes. With higher rates of differentiation (e.g.,

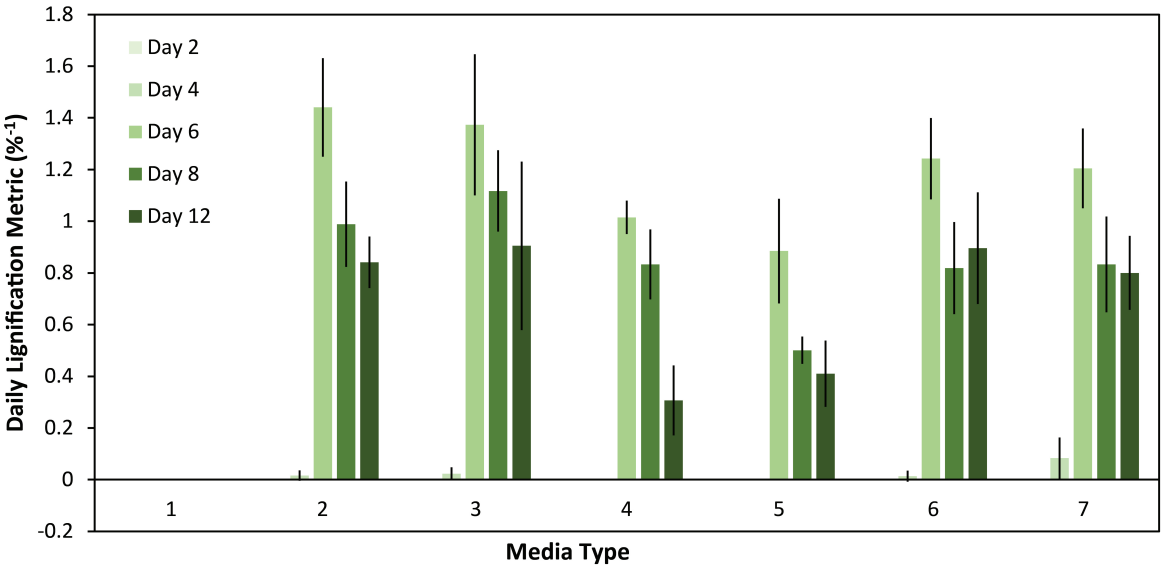

Figure 8: **Daily lignification metrics of *Z. elegans* cells in various media.** Lignification peaks at highest values for media treatments 2, 3, 6, and 7. This grouping includes media recipes which also resulted in maximized lignification during the original factorial experiment. N = 6 images per datum point.

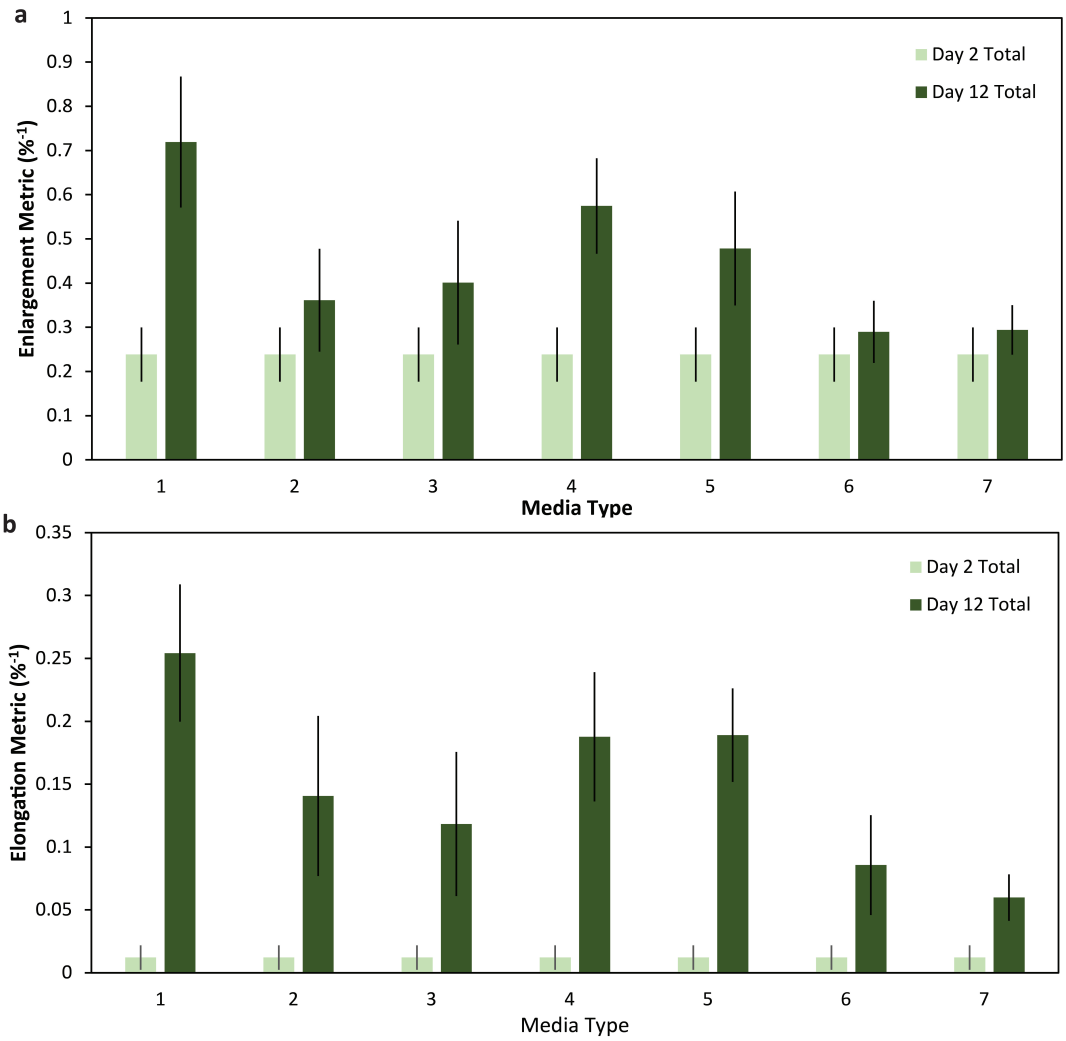

Figure 9: **Enlargement and elongation behavior of *Z. elegans* cells in various media.** (a) Low-hormone treatment 1 exhibits highest levels of enlargement as seen in initial experiments. (b) Higher levels of elongation tend to correspond to media types with lower levels of differentiation (e.g., Media 1, 4, 5) into tracheary elements for the selected media treatments. N = 6 images per datum point.

elevated lignification metric) in verification runs, corresponding enlargement and elongation occurrence is reduced, whereas the original data exhibited smaller lignification magnitudes with increased enlargement and elongation metrics. Interactions between these developmental outcomes should be considered in the design of material cultivation processes.

In summary, trends in hormone-responsive development are consistent across biolog-

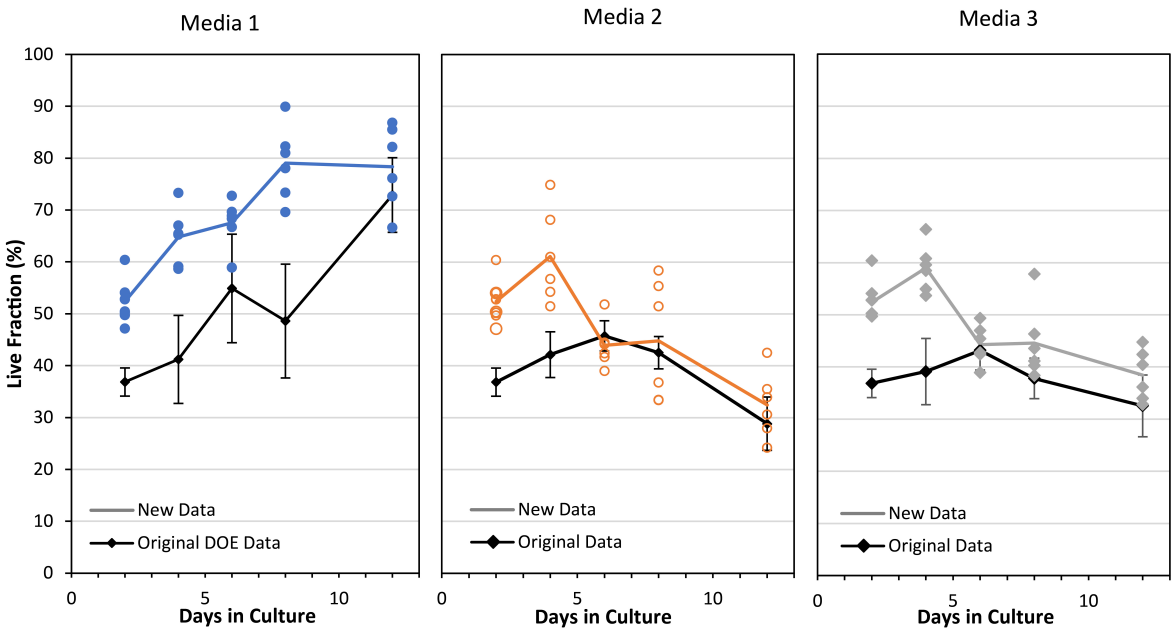

Figure 10: **Live fraction of repeat test points compared against original data.** Despite notably different starting points for the initial DOE and the verification samples, the live fraction metrics settle out to similar values by day 12 in culture. On the final day of these experiments, the new data and original data did not differ in a significant way for media 1,2, and 3 (with P=0.303, 0.376, and 0.122, respectively). Media numbers correspond to formulations listed in Table 4. N = 6 images per datum point.

ical samples. However, magnitude of response can be influenced by additional culture attributes. The data presented indicates that cell density and biological potency are potential "sensitizers" in the processs of hormone-induced differentiation. The modulation of these culture characteristics seemingly alters cellular receptiveness to differentiation under the right hormonal conditions. High rates of differentiation, seem to correspond to reduced culture potential for further cellular enlargement and elongation.

8.3 Effects of Media pH on Cell Development

Auxin-mediated cell elongation is believed to act, at least in part, by encouraging the release of cell wall-loosening factors, which may include hydrogen ions [52]. Wall-loosening factors are believed to promote wall compliance, enabling cell expansion and restructuring [52]. Therefore, hydrogen ion concentration in the growth medium, as reflected by

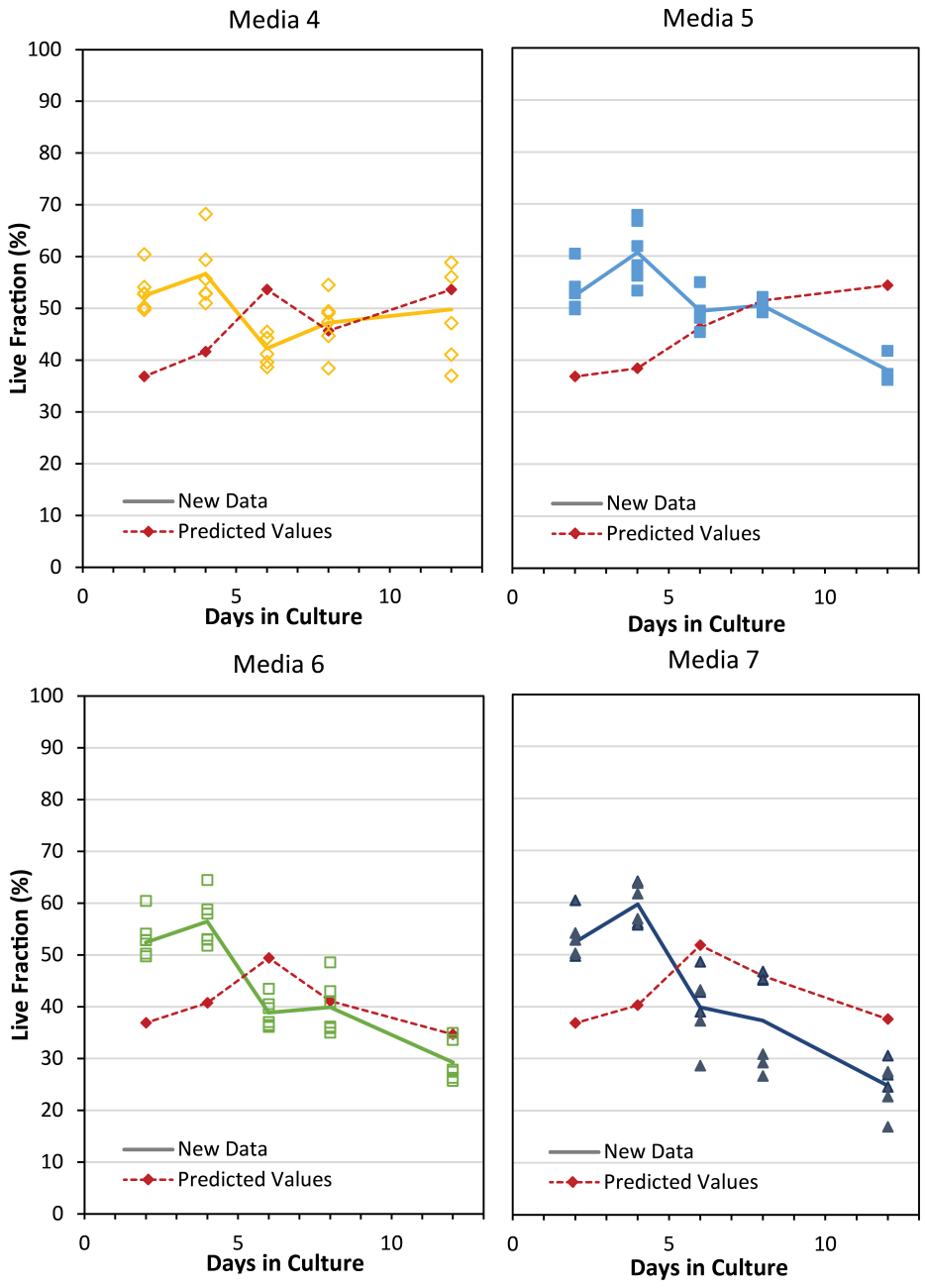

Figure 11: **Live fraction of cultures grown at various hormone-levels compared against predicted model data derived from previously reported factorial results.** Linearly-interpolated predicted values are good predictors for most of the media groups tested. Values at the extremes (e.g., media 5, 7), in regions where interpolated slopes were high, show some deviation from predicted values in the final days of culture. P-values for day 12 of New data compared with predicted values from a one sample t-test against the predicted mean for Media 4-7 are 0.3697, 9.74×10^{-4}, 0.02, and 0.0012, respectively. Media numbers correspond to formulations listed in Table 4. N = 6 images per datum point.

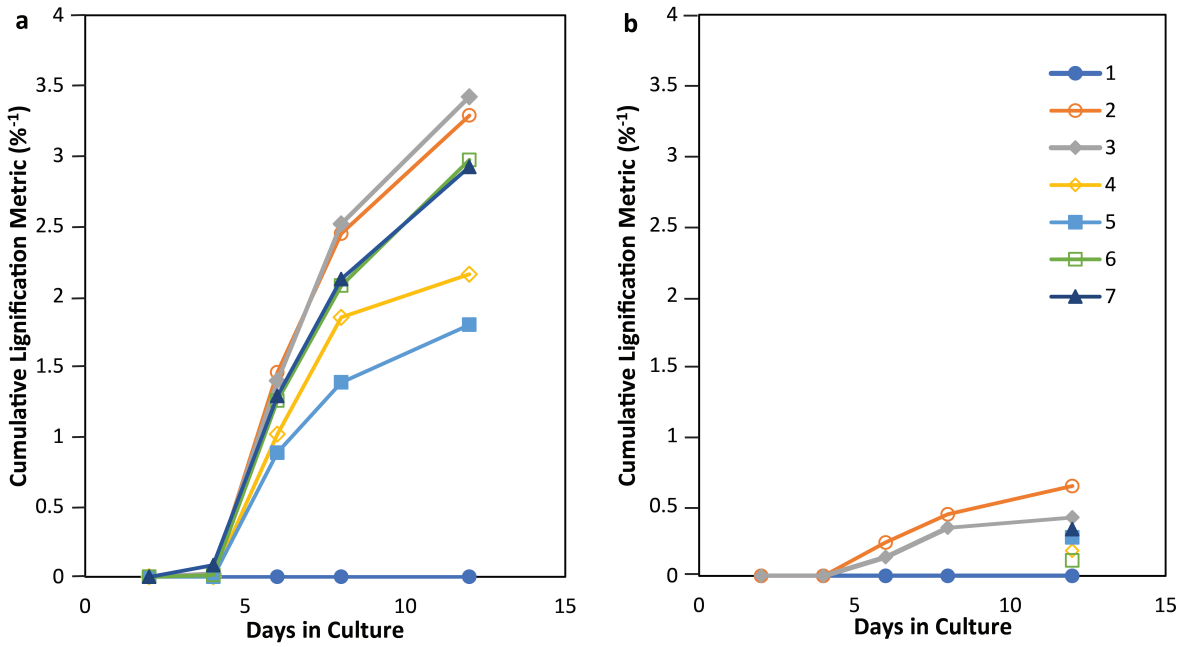

Figure 12: **Cumulative lignification metric of verification data (a) compared with initial data (b).** Across both original and verification runs, media 2 and 3 exhibit elevated cumulative lignification metrics, but metric magnitude is increased dramatically in verification data. N = 4 - 6 images per datum point.

pH, was similarly suspected to influence cellular development.

To investigate the effects of medium pH on cell development, *Z. elegans* cells were cultured in either maintenance media (Ze-M) or induction media (Ze-I) at one of 3 pH values (i.e., prepared at pH 5.22, 5.75, or 6.4 prior to a final autoclave sterilization). After a 48 hour acclimation period in which all isolated cells were cultured in low-hormone medium at pH 5.75, samples were transferred to treatment media and imaged periodically over the course of the subsequent 10 days. From the analysis of fluorescence micrographs, live fraction, lignification, enlargement, and elongation metrics were evaluated for each of the culture treatments. The data indicate that pH can be a driver of cellular development under some hormonal conditions.

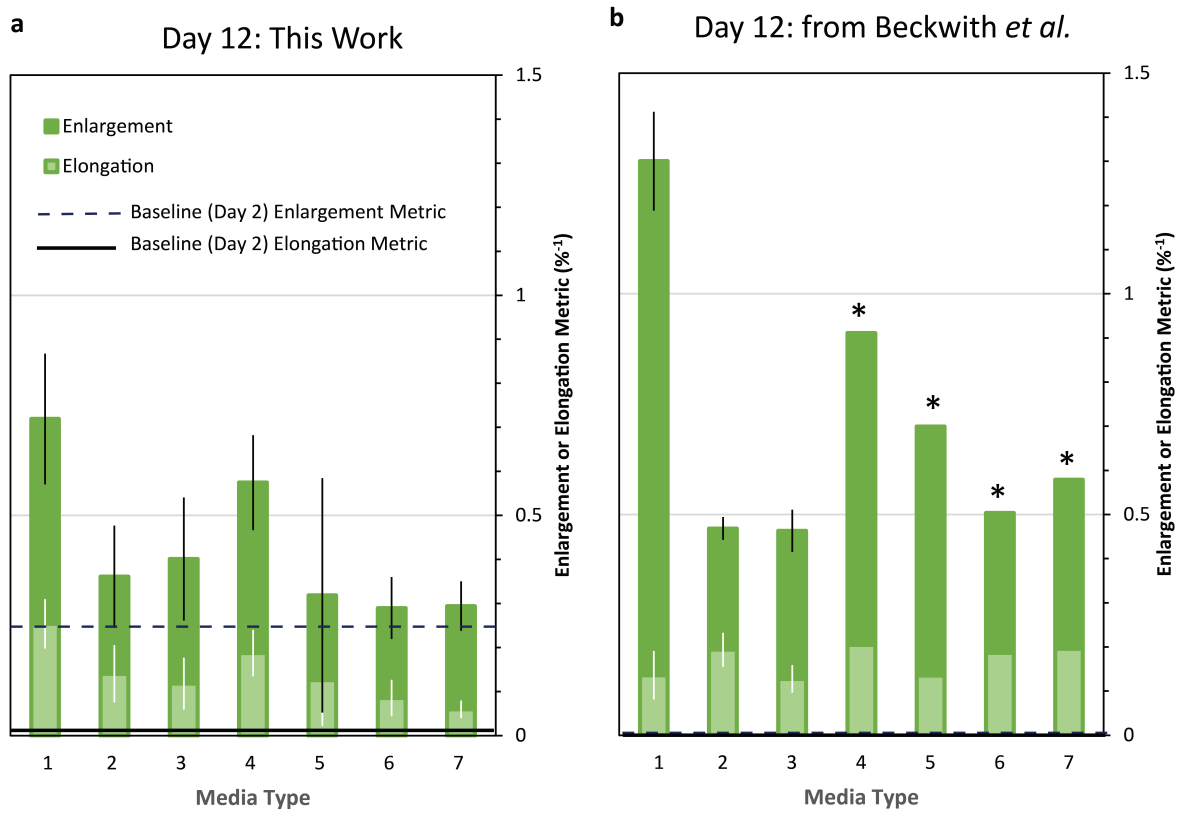

Figure 13: **Enlargement and elongation metrics alongside original DOE data for cell cultures on Day 12 (panels a and b, respectively) fed with media types 1-7 listed in Table 4.** Trends in enlargement and elongation remain similar across experiments, but magnitudes of response varied between experiments (e.g., absolute values for Media type 1 on day 12 vary significantly across experiments (P = 1.366×10^{-13}) and when net change across the culture period is taken into account, this difference is even greater). The net changes in enlargement and elongation metrics were smaller for this work than seen in original DOE data. One possible explanation for this is a difference in the biological pre-disposition of cells towards different developmental pathways. For example, the experiment which yielded panel *a*, saw reduced cell enlargement but exhibited higher lignification rates for differentiation-triggering media groups compared to original tests. Meanwhile, data from the original DOE generally conveyed larger increases in cell size compared to baseline Day 2 values over the culture period (*b*), but saw reduced lignification rates overall. It may be that innate responsiveness of cells to differentiation cues somehow inversely impacts morphological developments like enlargement and elongation. Asterisks indicate predicted values obtained through linear interpolation between original data points. Note that the same thresholding limits were used in the verification experiment as in the original experiment and the verification data saw a higher starting quantity of enlarged cells by the assigned limits. N = 4 - 6 images per datum point. Average baseline values for these metrics (obtained by analyzing cultures on Day 2) are plotted as horizontal lines.

8.3.1 Discussion of Experimental Results

In low, hormone maintenance media (Ze-M), pH had negligible effect on culture live fraction or lignification metrics, but did impact cellular enlargement and elongation. Live fraction for Ze-M cultures increased from a starting point of 36.4% at day 2 to a final value close to 80% (Figure 14). These results align with those of the factorial hormone experiment wherein low-hormone cultures similarly experienced a shift in live fraction from 36.8% to over 70% at the final time-point. Viability of low-hormone (Ze-M) cultures exhibited no significant differences in response to the altered pH levels, suggesting that the selected pH values were not independently detrimental to cell viability. For Ze-M samples at low pH levels, measured cells tended to be larger in size as quantified by enlargement and elongation metrics. Low pH Ze-M samples were significantly larger than medium or high pH samples ($P = 0.03$ and 0.016, respectively). Low pH Ze-M samples exhibited greater elongation than moderate pH samples ($P = 0.018$) which in turn, experienced significantly greater elongation than high pH samples ($P = 0.0095$) by day 12.

For cultures grown in high-hormone induction media (Ze-I), pH adjustments influenced both live fraction (Figure 14) and lignification metrics (Figure 15), but did not significantly impact enlargement or elongation. For Ze-I samples, live fraction trended downward after day 6 as levels of differentiation increased, settling out to values around 40%. This decline after day 6 is consistent with behavior seen in Ze-I cultures of previous experiments. In low pH Ze-I medium, declines in live fraction were greater than those seen in high pH samples on the final culture day ($P = 0.00062$). Correspondingly, low pH Ze-I cultures exhibited elevated lignification metrics for days 6, 8, and 12 when compared to high pH samples ($P = 0.00072$, 0.045 and 0.0013, respectively). These results are consistent with the observed inverse relationship between live fraction and differentiation. Adjustments to pH did not generate notable trends in morphological development for Ze-I cultures (Figure 16).

To summarize, within the physiologically tolerable range investigated, media pH was

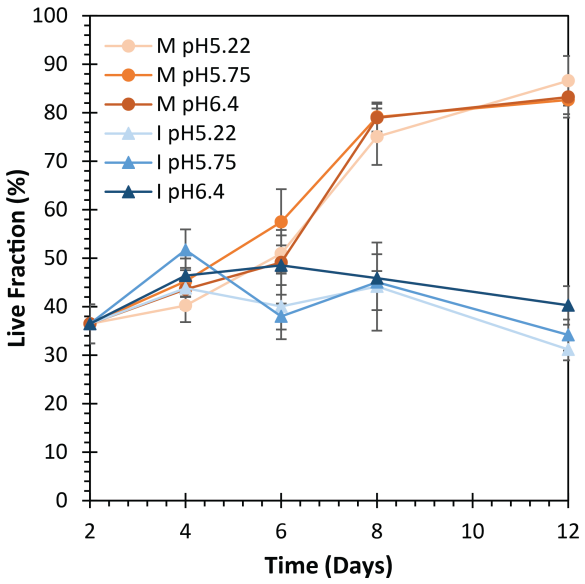

Figure 14: **Live fraction versus time in pH-adjusted culture.** Live fraction increases for cultures in maintenance media (M) for all pH levels, whereas live fraction remains low when cells are supplied with induction media (I). When cultured in induction medium, cultures yield lower live fraction for lower pH values in later culture stages. N = 4 - 5 images per datum point. This figure was published in Beckwith *et al.* [11]

seen to impact cellular development. The manifestation of these impacts varies with hormone concentration. At low levels of hormone concentrations, adjustment to pH altered the extent of cellular enlargement and elongation. At high levels of hormone concentration, pH alterations impacted differentiation rates (i.e., as measured by the lignification metric) and corresponding culture live fraction.

8.4 Effects of Initial Cell Density on Cell Enlargement and Elongation

Cell concentration can reportedly influence cellular development in liquid cultures [34]. Cell density is thus likely to play a critical role in the development of gel-based cultures.

Effects of cell density on development were quantified through the image analysis of gel cultures established at four starting cell densities and then monitored for a 14 day incubation period. Gel cultures were prepared at initial cell densities of 5×10^4, 1×10^5,

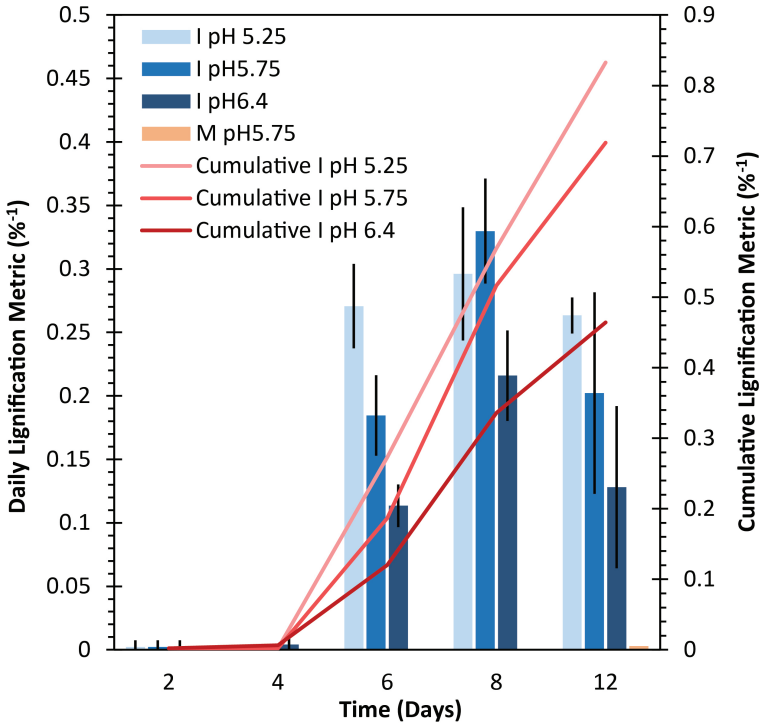

Figure 15: **Lignification versus time in pH-adjusted culture.** Daily lignification metric and a cumulative lignification metric (i.e., summed data of a given timepoint and all previous timepoints for a selected treatment group) versus time in culture. Daily and cumulative lignification metrics are highest for induction media (I) with the lowest pH while culture sustained in maintenance media (M) retains a lignification metric close to zero throughout the experiment. N = 4 - 5 images per datum point. This figure was published in Beckwith *et al.* [11]

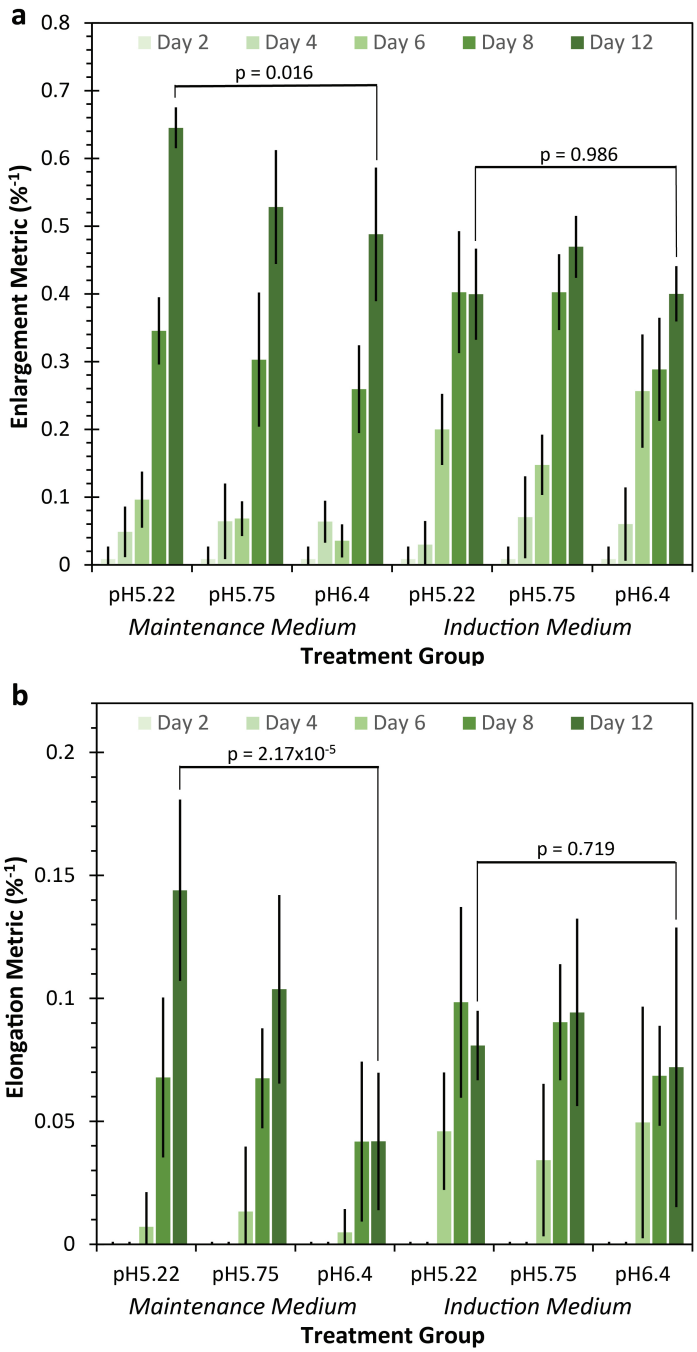

Figure 16: **Cell enlargement (a) and elongation (b) metrics versus time in pH-adjusted culture.** Cell enlargement and elongation increase with culture time and are influenced by pH when hormone levels are low. N = 4 - 5 images per datum point. This figure was published in Beckwith *et al.* [11].

2×10^5, and 4×10^5 $cells/ml$ (i.e., 1×, 2×, 4×, and 8× multiples of 5×10^4 $cells/ml$). For every time-point, two replicate gel cultures were prepared at each concentration and at least three independent images were captured and evaluated per replicate.

8.4.1 Discussion of Experimental Results

After 14 days in culture, cells seeded at higher initial cell densities exhibited increased cell size as quantified by both enlargement and elongation metrics (Figure 17). While differences between enlargement metrics were not significant at low densities (i.e., up to 1×10^5 $cells/ml$), pronounced enlargement was evident at higher cell densities. Enlargement metrics for cultures at 2×10^5 $cells/ml$ were higher than cultures at 1×10^5 $cells/ml$ (P=0.0097), and those at 4×10^5 $cells/ml$ were higher than cultures at 2×10^5 $cells/ml$ (P=0.0014). Similarly, with respect to elongation, differences between the two lowest density cultures were not significant. However, cultures at 2×10^5 $cells/ml$ and 4×10^5 $cells/ml$ presented higher elongation metrics, and thus longer cells, than lower density cultures at 1×10^5 $cells/ml$ (with P=0.0241 and P=0.011, respectively).

To confirm that the imaging methods provided a representative snapshot of the gel cultures in spite of their three-dimensional nature, total evaluated percent area (A_T) was plotted against concentration factor to check for linearity (Figure 18). The relationship between cell concentration and evaluated area was confirmed to be linear with R-squared values exceeding 0.98 when linear trendline intercepts were set to zero; setting the intercept as such reflects the state at which no cells are present and, therefore, the total percent cell area, A_T, is zero.

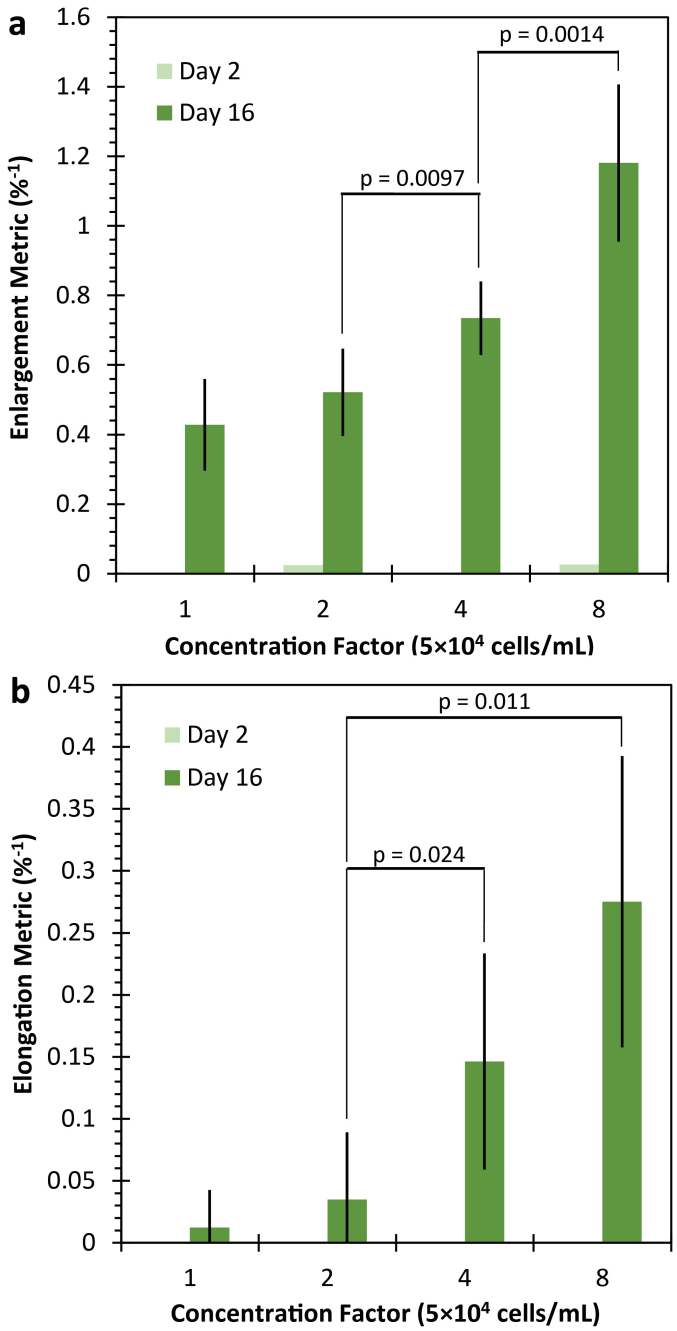

Figure 17: **Cell enlargement (a) and elongation (b) metrics versus initial cell concentration.** Enlargement metric and elongation metric increase with time in culture and with increasing initial cell density. N = 4 - 5 images per datum point. This figure was published in Beckwith *et al.* [11].

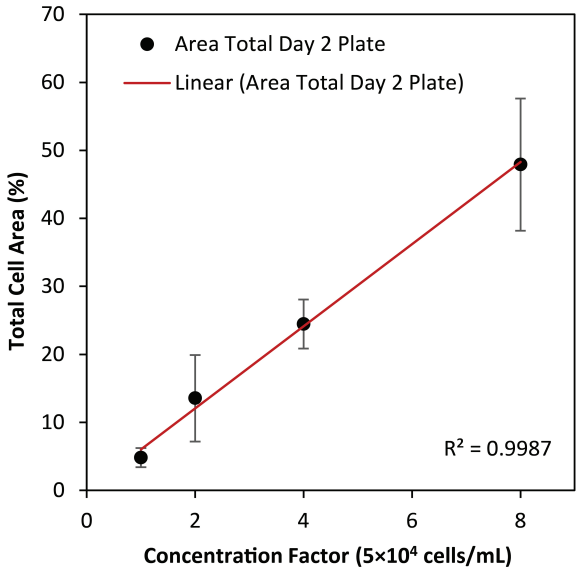

Figure 18: **Linear relationship between cell concentration and total evaluated area, A_T in dispersed gel cultures.** Total evaluated percent cell area, A_T, increases linearly with concentration factor. Thus, within the evaluated concentration ranges, the imaging methods provide a representative look at the imaged cell population. N = 6 images per datum point. This figure was published in Beckwith *et al.* [11].

8.5 Takeaways

- This section demonstrated the possibility of controlling cellular differentiation and morphological development through alterations to the culture environment – specifically, adjustments to auxin/cytokinin levels, pH, and initial cell density.
- With the proposed metrics (i.e., live fraction, lignification, enlargement, and elongation metrics), cell response to various culture environments was mapped for use informing culture setup to elicit desired growth characteristics.
- Trends quantified by developed metrics are repeatable across biological samples of *Zinnia elegans* – which speaks to the utility of the metrics and the reliability of the Zinnia cell response to the selected stimuli.
- Experimental results clarify relationships between the developed metrics (e.g., the inverse trends between live fraction and differentiation metrics, as well as the elongation and differentiation metrics) enabling thoughtful direction of growth.

9 Exploring Form Control of Grown Materials

Insights gained from experiments on cell growth in response to chemical cues informs the production of materials on a cellular level. In conjunction, the grown material can be tuned macroscopically to yield specified shapes. Here, bioprinting and casting of structured growth environments enable the production of monolithic forms and materials at sizes which are not naturally possible.

The process of material growth consists of the following four steps: cell feedstock generation, incorporation of cells into structured growth environment, cultivation, and dehydration. In the case of bioprinting, cell-laden, nutrient rich scaffolds were deposited using a syringe-based extrusion system (see Chapter 7). Because required nutrients and hormones are incorporated within the scaffold itself, this fully contained setup requires little intervention after deposition. The scaffold can sustain growth through differentiation and to confluency without requiring supporting continuous perfusion systems. Cultures can survive and continue to grow for months after printing (Figure 19) with the occasional addition of liquid medium to prevent premature dehydration. Because viability is not required beyond the point of confluency, this approach provides a simple means of cultured plant material production. The employment of nutrient-rich gel as a medium for tissue-like growth is inspired by culture methods put forth by Ludwig Bergmann in the 1960's. Bergmann demonstrated the immobilization of single plant cells in a thin layer of gel media for the purpose of monitoring cell division and colony development [54]. Through modifications to foundational techniques, advancements in this work allow for not only the prolonged immobilization and survival of cells in gel, but the directed growth and development of gel-based cultures to produce tunable materials in desired shapes.

After a cultivation period, samples were rinsed and carefully transferred to a desiccator for drying between two teflon-wrapped surfaces. During the drying process, the samples experienced some shrinkage—the amount of which seemed to vary with extent and type of growth.

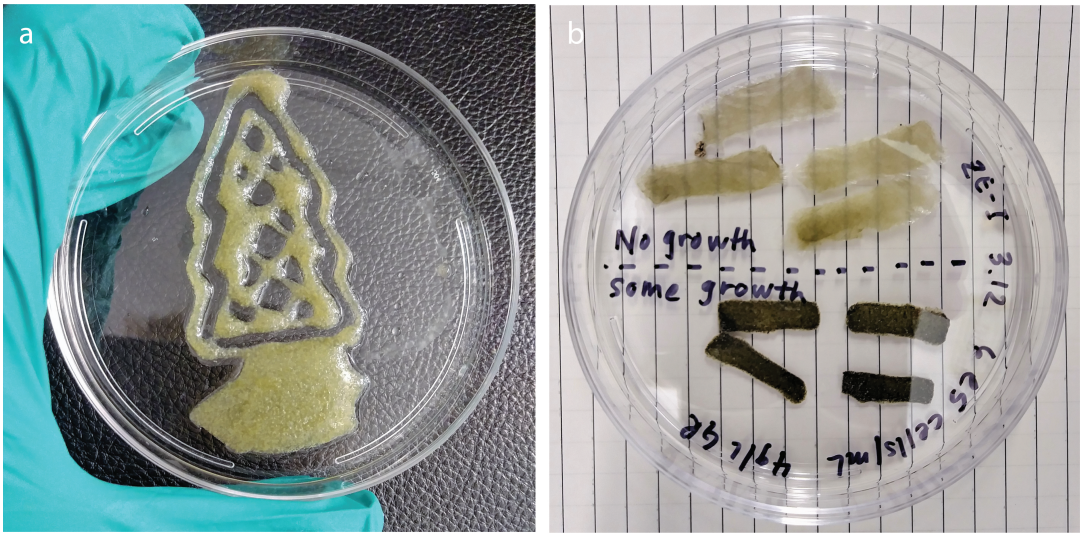

Figure 19: **Long-term growth is possible in perfusion free cultures.** (a) A healthy, hydrated, bioprinted culture after 3-months of cultivation retains a green hue and has become relatively opaque in appearance. Excess cell-laden gel has been deposited around the outskirts of the printed structure and also continues to support growth. (b) After dehydration, the difference between samples which do not grow (top) and those that do (bottom) is stark. Printed samples without growth remain translucent while successfully grown samples are thicker, opaque, and experience more notable lateral shrinkage in the print plane.

A number of culture forms were prepared and cultivated in order to produce net-shape plant materials (Figure 20). While these initial samples are small in size, being printed into a 10-cm petri dish, they nevertheless yield materials at large scales compared to similar tissue-like materials grown in a whole plant. Figure 21 depicts a cross-section of a grown, dehydrated material sample compared to a cross-section of a Zinnia-stem which was halved and dried flat.

For the purposes of these early investigations into net-shape plant material production, grown structures were kept to planar, relatively thin configurations. However, production of larger samples will likely require cell survival in thicker gel culture environments. To investigate survival at increased culture dimensions, gelled cell cultures were plated at various gel depths (distances from the gel surface) on culture day 2 in 24-well plates (Figure 22a) and allowed to grow for 32 additional days. For depths evaluated (i.e., 2.5, 5, 8.7 mm atop a 2.5 $mm-thick$ cell culture), there was no apparent

impact on live fraction after 32 days in culture gel culture (Figure 22b) with P ¿ 0.18 for all sample-to-sample comparisons on day 34. All samples exhibited an increase in live fraction from initial seeding to final evaluation. These results indicate that growth of thicker structures is possible.

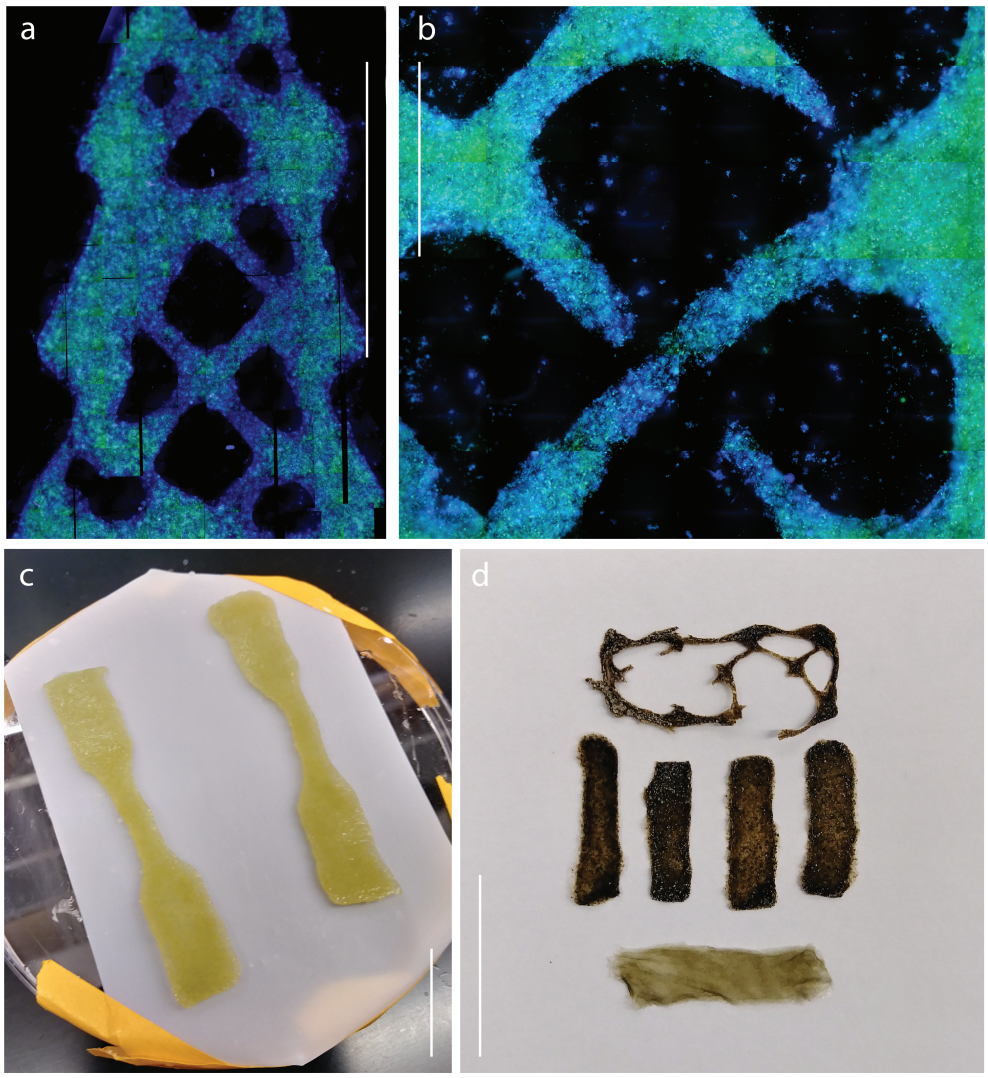

Figure 20: **Grown materials can be produced in forms not naturally available.** Assorted bioprinted, cultivated plant materials: (a) a stitched, two-channel fluorescence micrograph of a tree-shaped print (black lines are a result of positioning errors during imaging) (b) a stitched, two-channel fluorescence micrograph of lattice-like culture (c) dog-bone structures after transfer to drying plate, (d) dehydrated samples with growth (dark samples) and without growth (bottom sample). Small features, on the order of 1 mm, are achievable, but delicate (top). Scale bars in a, b, and c represent 2.5 cm. The scale bar in panel b represents 5 mm.

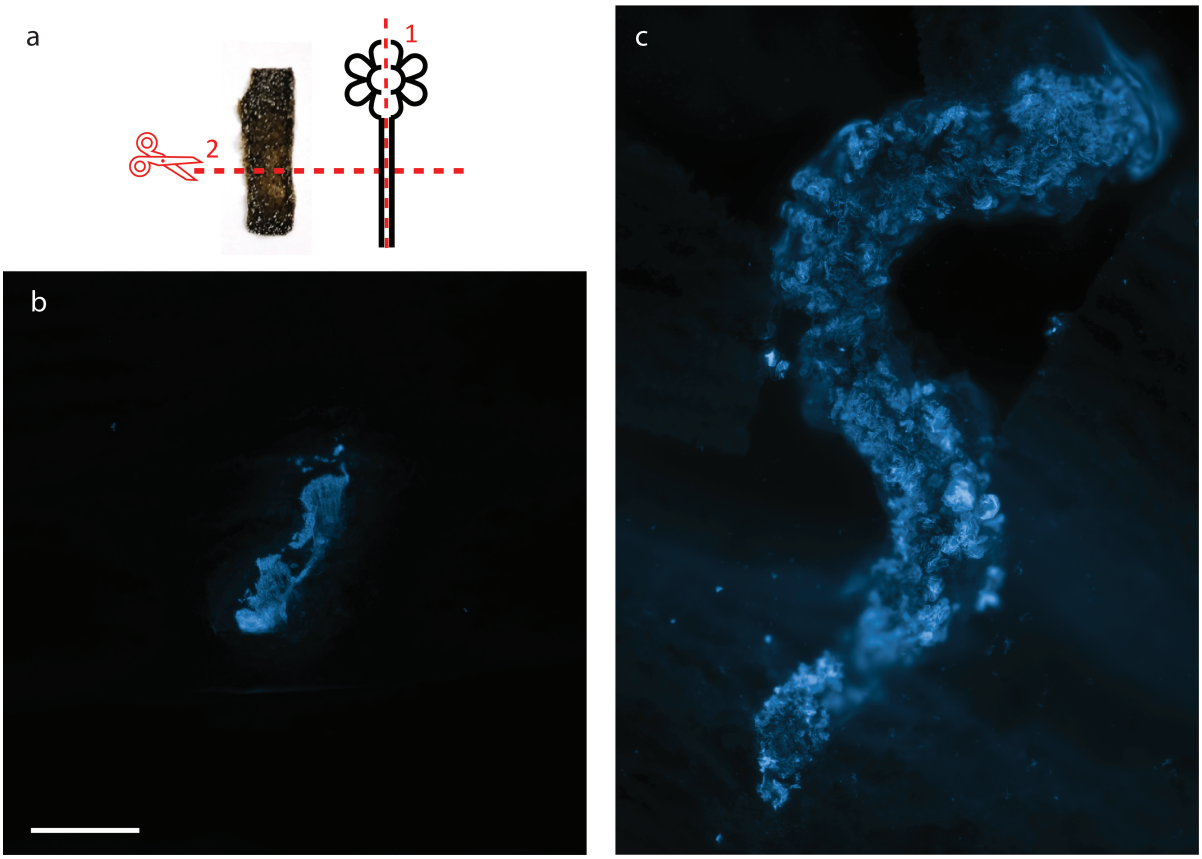

Figure 21: **Grown materials can be produced at scales larger than naturally achievable.** (a) Materials were sectioned as shown. Stem samples were halved lengthwise (cut 1) and dried flat before fixing in wax and sectioning with a microtome along the indicated cut 2. Dehydrated cultured samples were fixed in wax and sections and sectioned as indicated in cut 2 and stained with CW to illuminate plant cell wall material. (b) A cross-section of a halved and dried Zinnia stem– which is small in scale compared to the sizes accessible by the proposed direct-material growth method for the same growth time. (c) A cross-section of a grown material sample sliced along the shortest dimension. Two images are stitched together to visualize the whole extent of the sample. The sample curvature is a result of the fixing, slicing, positioning, and staining processes. Both samples are pictured at the same magnitude. Scale bar equals 500 micrometers.

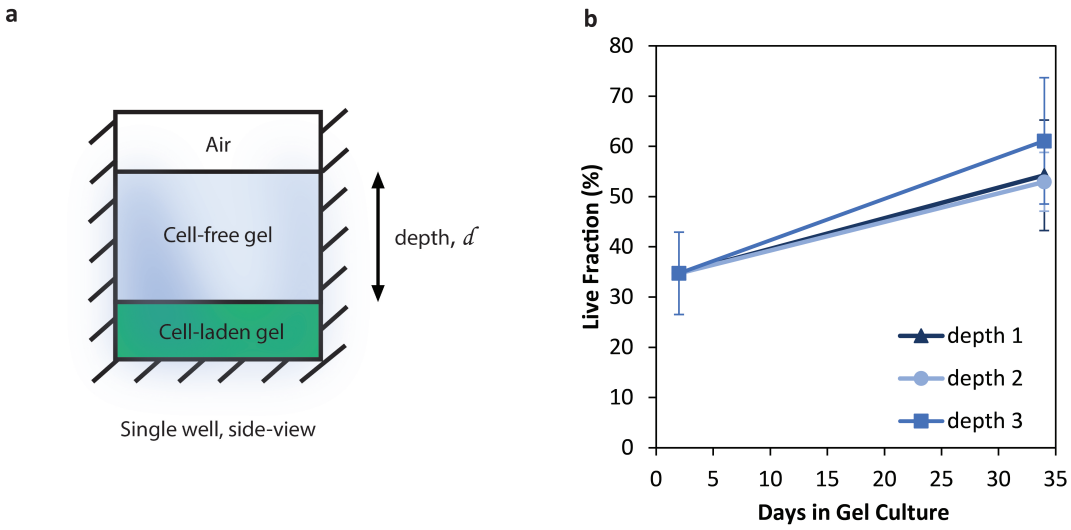

Figure 22: **For cell cultures grown under gel depths up to 8.7mm thick, cell survival was not impacted.** (a) Cell-free gel media was deposited and gelled atop a cell-laden gel media mixture 2.5 *mm* thick. (b) Cells were cultured for 32 days beneath cell-free gel layers of various depths. Gel depth, d, was set to 2.5, 5, and 8.7 *mm* for depths 1, 2, and 3, respectively. Gel depth did not impact cell viability within the tested range. On day 34, P = 0.80, 0.180, 0.34 for sample-to-sample comparisons of depths 1 – 2, depths 2 – 3, and depths 1 – 3, respectively. N=6 samples per datum point.

9.1 Takeaways

- Scaffold structure, which can be controlled through selective deposition, bounds and guides plant material growth.
- Scaffold-guided growth enables production of plant materials in *forms* otherwise unavailable using traditional cultivation methods.
- Scaffold-guided growth enables production of plant materials at *sizes* otherwise unavailable using traditional cultivation methods.
- Cells can survive long-term even in thicker structures, more than 8.7 *mm* from the gel surface for at least 32 days.

10 Characterization of Grown Materials

To assess whether differences in cell growth as modulated by environmental culture parameters map to emergent material characteristics, the mechanical, physical, and microstructural properties of cultivated samples were investigated. Results indicate that both macro-level and micro-level properties are significantly impacted by selected media formulation. Samples grown in two culture formulations, Ze-M and Ze-I, were evaluated. Ze-M media is intended to support growth and proliferation without differentiation of cells, whereas Ze-I media is formulated to induce cells to form vascular cell types with thickened and lignified secondary cell walls. Natural zinnia samples were prepared from the stem of the Zinnia plant that was harvested at the same age as cultured samples. While stem samples were useful in preparing cross-sections for microstructure visualizations, the samples were too small and lightweight to be accurately measured using the physical and mechanical measurement techniques available for this work—evidencing how lab-grown tissue techniques enable faster growth of materials in useful forms.

10.1 Mechanical Evaluation of Grown Materials

Mechanical properties of grown samples were assessed using dynamic mechanical analysis. Mechanical properties were found to change with variations in media hormone-levels.

10.1.1 About Dynamic Mechanical Analysis

Dynamic mechanical analysis (DMA) enables the non-destructive assessment of mechanical properties through the application of a small-amplitude, oscillating strain and evaluation of sample response. Unlike uniaxial testing, in which samples commonly undergo extensional strain beyond the Hookean regime and to failure, dynamic mechanical testing is usually performed entirely within the Hookean or linear viscoelastic regimes of materials subjected to oscillating stresses or strains [55]. In the employed DMA setup, a test sample is positioned between two fixtures: one stationary, and another which imposes a time-dependent, sinusoidal strain. The resulting time-dependent stress is simultaneously

monitored by quantifying the torque generated on the stationary fixture [56] (Figure 3).

The relationship between applied strain and simultaneously recorded stress data provides insights into the mechanical properties of the tested sample. The phase shift between the two curves, is used to determine the storage modulus (ratio of elastic or in-phase stress to strain) and loss modulus (ratio of viscous or out-of-phase stress component). Effectively, the storage modulus represents the material's elastic behavior or stiffness whereas loss modulus relates to the material's capacity to dissipate energy. It should be noted: the storage modulus and Young's modulus are conceptually related but are not the same[e][57]. When storage modulus exceeds loss modulus, this indicates predominantly elastic behavior. For perfectly elastic materials, with stress and strain linearly related, the stress strain curves are in phase ($\delta = 0$) as the materials immediately return to their original form upon removal of applied strain. Purely viscous materials exhibit a phase shift of 90 degrees ($\delta = \pi/2$). Viscoelastic materials experience phase shifts between these extremes ($0 < \delta < \pi/2$) [58].

DMA allows for testing of smaller samples than those typically recommended for ASTM compliant uniaxial tensile tests. For torsional DMA tests, small rectangular or cylindrical samples are recommended. According to PerkinElmer, a manufacturer of DMA devices, width is not a critical dimension and geometry is ultimately constrained by the ability to clamp the sample uniformly. DMA manufacturers recommend a 5-mm wide sample with a test length (i.e., clamp separation) of 5 – 10 mm [59].

10.1.2 Identifying Testing Bounds

Preliminary tests are necessary to identify appropriate experimental bounds for DMA measurements on unknown materials. Determination of appropriate parameter settings ensures that testing is performed non-destructively [56]. The typical procedure for establishing these test settings includes execution of a strain sweep to identify critical strain and a frequency sweep to determine the frequency-independent regime of material

[e]In the particular configuration used for evaluations of plant materials in this work, samples are subjected to a small amplitude, sinusoidal twisting action making inferences about elastic modulus even more difficult.

response.

A strain amplitude sweep performed at constant temperature allows for the identification of the region where modulus values are independent of strain amplitude [60]. This region is bounded by the so-called 'critical strain' beyond which, amplitude-independence breaks down. Once this range of strain is identified, all future tests are performed at strain amplitudes within this linear viscoelastic region. Strain sweeps were performed on the cultivated materials of interest and critical strains were identified as indicated in Figure 23. A suitable strain amplitude within the linear strain-independent regime was selected and held constant for all subsequent tests.

A frequency sweep performed at a constant temperature provides information on the time-dependency of the system response. A frequency sweep was performed to ensure that measured moduli remained consistent across the possible measurement spectrum and anomalous, frequency-dependent artifacts did not skew the reported results. Fre-

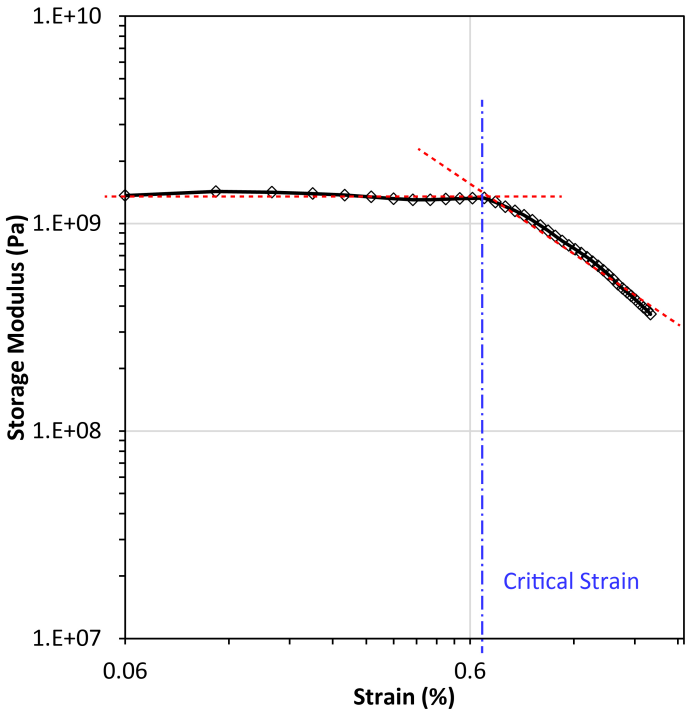

Figure 23: **Strain sweep on dehydrated sample.** Sample response is nearly independent of strain until the critical strain is reached. All subsequent tests were conducted below the critical strain value.

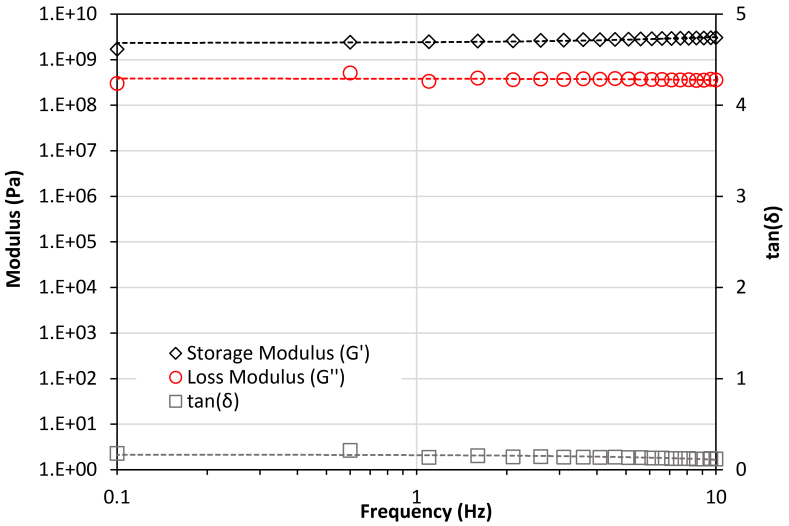

Figure 24: **Frequency Sweep of Dehydrated Cell-Free Sample.** A frequency independent response indicates that the sample behaves elastically within the tested regime.

quency sweeps performed on cultivated materials demonstrated frequency-independence at the examined settings (Figure 24). This behavior is consistent with DMA theory and the current understanding of dehydrated, cultivated materials. In a system where molecules are strongly associated (i.e., as in a solid system), the storage and loss moduli are expected to be independent of frequency. Other notable features of the acquired data: elevated storage modulus relative to loss modulus and a low loss modulus indicate a predominantly elastic system, as does a low $\tan(\delta)$. Thus, preliminary DMA data properly indicate the produced materials are solid, elastic materials.

The effect of sample length (i.e., clamp separation distance) on modulus measurements was evaluated to identify appropriate length settings and understand the influence of this parameter on modulus measurements. A sample evaluated at four clamp lengths show that moduli values are nearly constant at low clamp distances. At higher sample lengths, absolute moduli values exhibit some decline, although the relative values of storage and loss moduli, as represented the $\tan(\delta)$ remains constant (Figure 25). For purposes of comparing modulus values across various sample types, subsequent measurements were all performed at a constant length of $5mm$—a clamp distance which meets

DMA manufacturer recommendations, and which falls within the range of low modulus sensitivity to sample length.

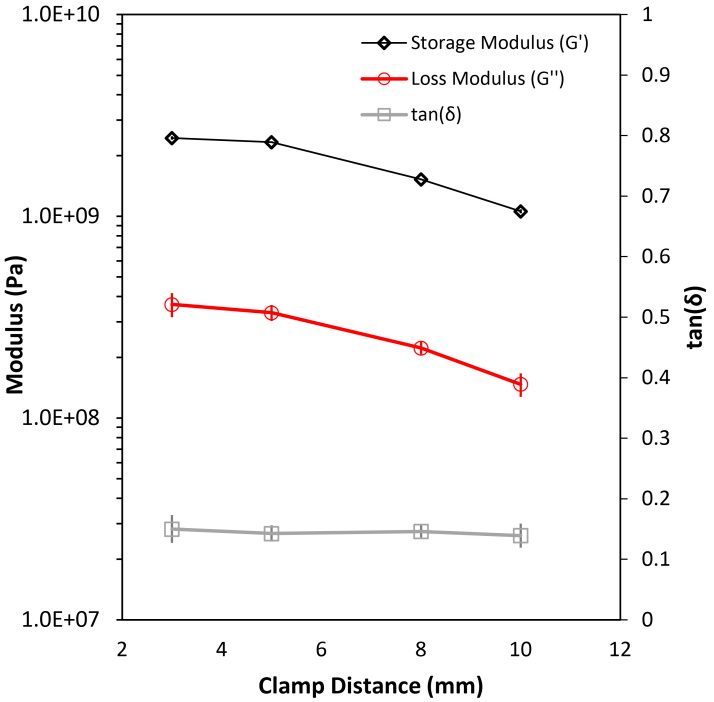

Figure 25: **Effect of clamp length on modulus measurements.** At increased distances between clamps, both storage and loss moduli are reduced, however, the ratio of the two reflected by the $tan(\delta)$ value remains constant. Subsequent tests were performed at 5mm clamp lengths.

10.1.3 Mechanical Properties of Cultivated Materials

For cellular materials cultivated under various growth conditions, strain-controlled DMA was performed to assess mechanical properties. Rectangular samples were prepared in either Ze-M (low hormone maintenance) or a higher hormone induction medium by means of bioprinting, incubation, and subsequent dehydration. Samples were generated on the same date with the same cellular feedstock and incubated for the same duration before dehydration.

Varying media compositions did result in significant differences in the resulting storage modulus of cultivated samples. The storage modulus values of differentiated Ze-I

samples were higher than measured storage modulus values for undifferentiated Ze-M samples (P = 0.033) (Table 5). However, the reason for this observed difference is not immediately obvious. Beyond the presence of stiffened, vascular-type cells, final material density, plant material fraction, and microstructure (i.e., cellular morphology and entanglement) can all contribute to macroscopic mechanical properties. The next sections explore these material characteristics and bring additional clarity to the initial DMA results. A measurement of dehydrated gel samples without plant materials is included for reference (Table 5). Storage modulus for gel is notably higher than grown plant samples; this is likely due to several factors including increased sample density as a result of reduced porosity and compositional differences, and natural stiffness of the single-phase gel material being higher than the stiffness of cultivated plant matter. Cell-free, gel materials are a useful reference for calibration, but are perhaps not useful benchmarks of progress towards *in vitro* plant material production. To contextualize the results presented in Table 3, available data on properties of natural plant materials are helpful references. Reported storage modulus values for woods have been reported in the range of 300 – 1200 MPa [61, 62], although exact values can vary with testing apparatus, setup, and sample grain orientation. In any case, DMA measurements for lab-grown samples appear to correspond well to the storage modulus measurements for natural tissues. While the shifts to storage modulus that result from tuning culture environment cannot yet be precisely attributed to a specific cause, the presented DMA results provide a compelling indication of the tunability of cultured materials by simple modifications to controllable system inputs.

Table 5: DMA Results for cultures grown in Ze-M maintenance medium and Ze-I induction medium and for prepared gel samples without cells. Values represents the average of at least 15 measurements for each of N=3 samples per treatment group.

Medium	**Storage Modulus (MPa)**	**Loss Modulus (MPa)**	$tan(\delta)$
Ze-M	138.3 ± 57.4	8.365 ± 4.47	0.065 ± 0.031
Ze-I	404.7 ± 146.9	16.0 ± 11.1	0.037 ± 0.014
Gel, No Cells	1451.0 ± 645.7	164.88 ± 127.6	0.100 ±0.002

10.2 Physical Measurements

Changes to mass and volume were evaluated for samples cultivated under various growth conditions. This data is also used to examine sample density, which was found to differ between cultures grown in altered media formulations.

10.2.1 Sample Masses and Densities

In addition to altering cell types, the different media formulations also impact the extent of culture growth (i.e., final amassed plant material) and the resulting cell morphologies. Materials grown in a Ze-M media base exhibited the largest gains in accumulated plant mass (Figure 26a). As previously noted, in cell populations induced to differentiate into tracheary elements (Ze-I cultures), rapid transformation and cell death leaves behind a smaller population of cells with the capacity for continued growth. These Ze-I samples thus tend to amass a smaller quantity of plant material compared to samples formulated from maintenance media. Interestingly, despite the greater plant mass accumulation in Ze-M samples, density is reduced compared to both Ze-I samples and samples without growth (Figure 26b).

Looking at the mass and volume changes as a percentage change, data for both Ze-M and Ze-I samples again demonstrate notable increases in both mass and volume relative to cell-free and growth-free controls (Figure 27). However, Ze-M samples exhibit proportionately larger changes of volume compared to mass, with a volume increase nearly four times larger than mass increase. By contrast, Ze-I samples exhibit a volume increase not quite two times larger than mass increase. These unbalanced ratios between mass and volume gains indicate underlying differences in the microstructure of the produced materials (further explored in Section 9.3).

The observed shifts in both mass and density convey a dramatic accumulation of plant matter. Characterized samples were seeded at an initial cell density of 6×10^5 $cells/ml$ and allowed to grow for 3 months. The resulting plant material accumulation generated substantial shifts in physical characteristics and measured modulus values. By contrast,

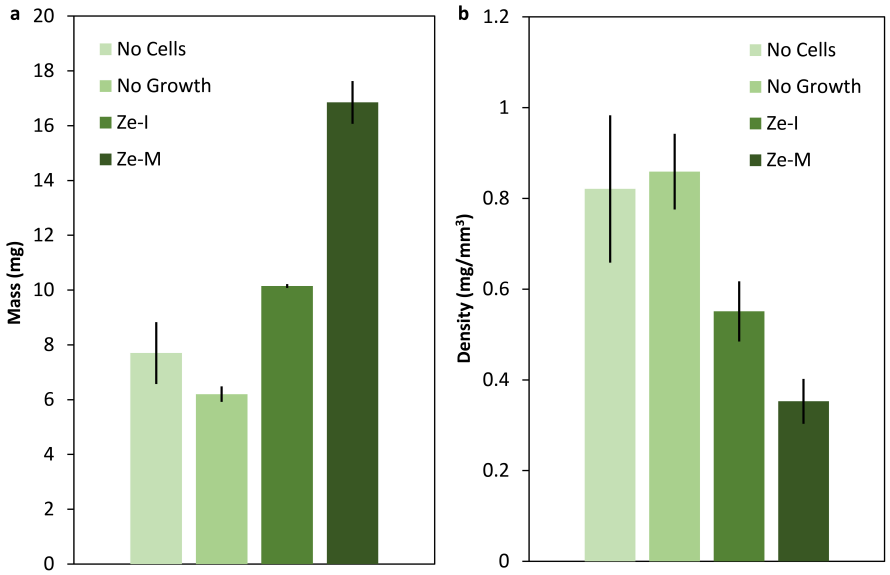

Figure 26: **Mass (a) and density (b) of samples cultivated in different media.** Samples grown in Ze-M medium experience the greatest increase in mass, and the greatest reduction in density. Both Ze-I and Ze-M samples exhibit notable changes in mass and density compared to cell-free and growth-free controls. Comparisons of Ze-M sample mass/density to No Growth and No Cells samples yielded P-values of 0.017/0.060, 0.003/0.018, respectively. Comparisons of Ze-I sample mass/density to No Growth and No Cells Samples yielded P-values of 0.003/0.055, 0.092/0.161, respectively. Samples were seeded at an initial density of 6×10^5 $cells/ml$ and cultivated for 3 months prior to dehydration. N=3 - 4 samples per treatment group.

small shifts in cell density have negligible impact. To illustrate, samples prepared at densities between 0 and 1×10^6 $cells/ml$ were prepared, dehydrated without allowing for additional growth, and characterized by the DMA and physical measurements outlined. These variations in cell content had no discernible impact on any of these parameters (Figure 28, Table 6).

10.2.2 Plant and Gel Mass and Volume Fraction

Using the acquired physical measurements, plant mass fraction and plant volume fraction estimates were calculated for the final materials. The contribution to final volume and mass by the non-living scaffold was assumed to be constant. In terms of both volume and mass fraction, samples grown in Ze-M medium resulted in the largest acquisition of plant

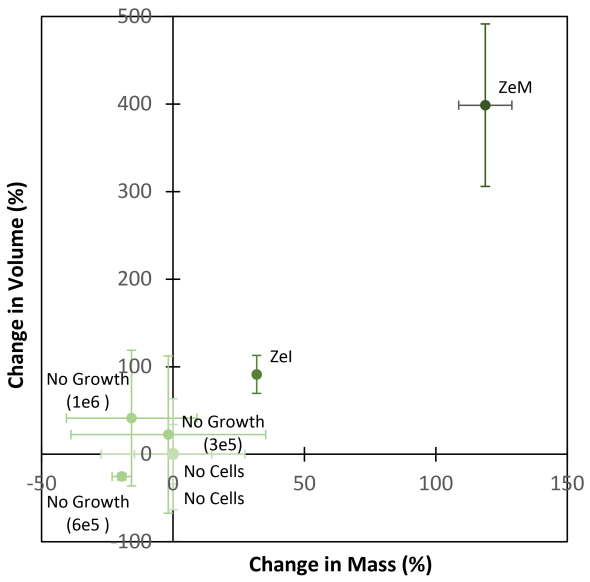

Figure 27: **Percent increases in mass and volume of samples grown in various media compared to cell-free and growth-free control.** Samples cultivated in Ze-M exhibit a volume increase nearly four times larger than mass increase. Meanwhile, samples in Ze-I exhibit a volume increase not quite two times larger than mass increase. Grown samples were seeded at an initial density of $6{\times}10^5$ $cells/ml$ and cultivated for 3 months, measurements were also made for growth-free samples prepared at various cell densities: $1{\times}10^6$, $6{\times}10^5$ $3{\times}10^5$ $cells/ml$. N=3 - 4 samples per datum point

Table 6: Summary of DMA Results for growth-free samples at various cell densities, without long-term incubation. N=3 grown samples per reported average.

Cell Density ($10^6 cells/ml$)	**Mass** (mg)	**Density** (mg/mm^3)	**Storage Modulus** (MPa)	**Loss Modulus** (MPa)
0	11.0 ± 3.0	1.63 ± 0.86	1331.8 ± 849.2	231.5 ± 153.2
0.3	10.8 ± 4.1	1.47 ± 0.84	840.2 ± 507.8	54.5 ± 7.7
1	9.27 ± 2.7	1.21 ± 1.2	1353.3 ± 1392.3	111.0 ± 189.2
Stem	-	-	7686.1 ± 7554.8	247.9 ± 289.7

material. Both sets of grown samples, in Ze-I and Ze-M media, exhibited marked increases in volume and mass fractions from both cell-free and growth-free controls (Figure 29).

Plant mass and volume fractions were calculated relative to the average respective measurement of the cell-free control:

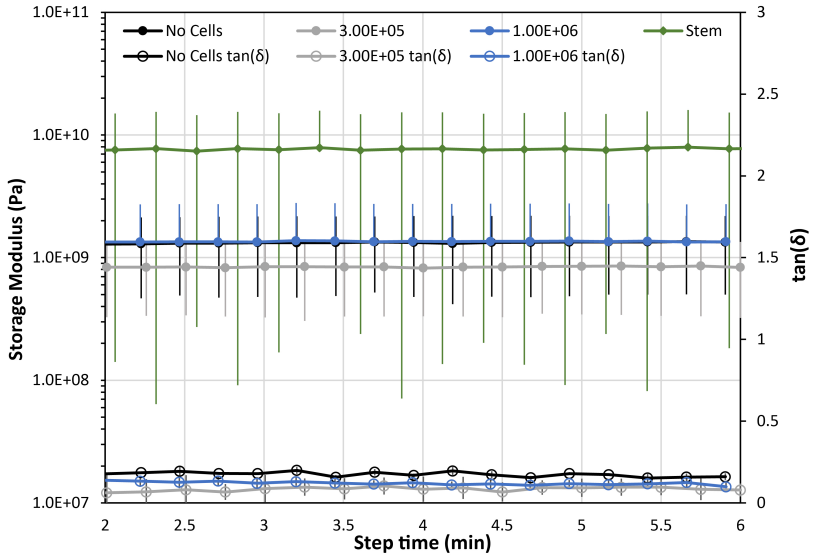

Figure 28: **Effect of changes in initial cell density on growth-free samples.** Samples were seeded at an initial density of 0, 3, or $10{\times}10^5$ $cells/ml$ and subsequently dehydrated and tested without allowing for further growth. Variation in cell density within the tested range did not significantly affect mechanical properties. For comparison, properties of halved and dried young Zinnia stems were also measured. N= 3 samples per treatment group.

$$M_{p,i} = 100\% \times (m_i - \overline{m_{ctrl}})/m_i \tag{5}$$

$$V_{p,i} = 100\% \times (V_i - \overline{V_{ctrl}})/V_i \tag{6}$$

where $M_{p,i}$ represents plant mass fraction for sample i with mass, m_i, relative to average mass of cell-free controls, $\overline{m_{ctrl}}$ and $V_{p,i}$ represents plant volume fraction for sample i with volume, V_i, relative to average volume of cell-free controls, $\overline{V_{ctrl}}$.

Because of small sample numbers, an imperfectly controllable printing process, and potential for inaccuracies in input variables (i.e., sample length, width, thickness, mass), standard deviation is relatively high for these volume fraction/mass fraction measurements. The intention of this data presentation is not to convey exact values, but to depict larger trends and benchmark current progress. Again these results reiterate the substantial increase in plant matter compared to no-growth and cell-free controls. The

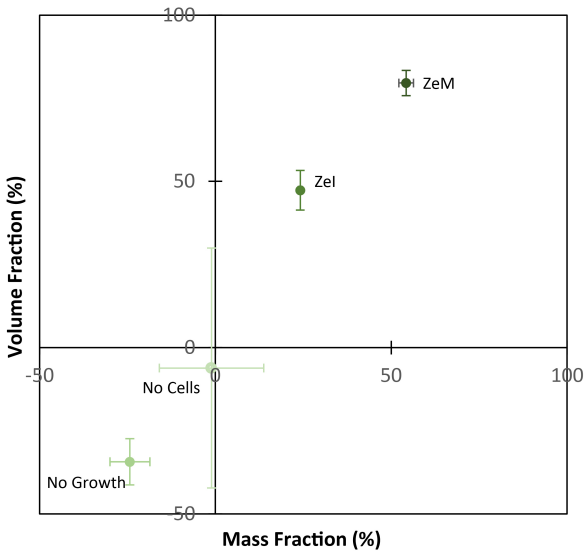

Figure 29: **Calculated mass and volume fraction of grown materials in various media.** Samples grown in Ze-M medium experience the greatest increase in mass and volume fraction. Both Ze-I and Ze-M samples exhibit notable changes in mass and volume fraction of plant material compared to cell-free and growth-free controls. Samples were seeded at an initial density of 6×10^5 $cells/ml$ and cultivated for 3 months prior to dehydration. N = 3 samples per datum point.

maintenance media indicates a higher plant material fraction in comparison to the induction media, which experienced less extensive growth.

10.3 Microstructure Visualization

Cellular morphology, in addition to cell wall make-up, can impact the dehydrated material microstructure—affecting material density and apparent response to applied strains. Material cross sections were visualized under a microscope to interrogate residual cell forms in dehydrated samples. Cultivated materials fixed in paraffin wax, sectioned with a handheld microtome, and stained with fluorescent cell wall markers. In the resulting fluorescent micrographs, structural differences are evident between samples which did and did not experience growth as well as between materials grown in different media formulations (Figures 30, 31).

The difference between sample microstructures is stark. In samples without growth,

cells are discrete, flattened structures with no interconnectedness. By contrast, grown samples are notably thicker and contain a higher proportion of visibly fluorescing plant wall material. Ze-M samples yield an open microstructure, with rounded cells retaining their shape upon dehydration. This helps to explain the substantial volume increases seen in Ze-M materials relative to controls. In Ze-M samples, opportunity for interconnectedness or entanglement is reduced by the nature of the predominant, round cell shape. On the other hand, Ze-I samples exhibit a tightly-packed network of plant material with a variety of cell configurations which could lead to increased interlocking of the plant material phase. The difference in measured mechanical properties is likely in part due to these changes in observed cell-to-cell connectivity. Figures 30 - 32 also include cross-section images of a Zinnia stem which has been halved and dried for comparison. The stem shown comprises multiple tissue types, but the vascular tissue of interest is visible when lignin is fluorescently labeled as well. Naturally the stem presents denser, more structured growth. However, xylem tissue is localized to only small regions of the stem and the overall form of the stem sample is thinner and less uniform than samples grown by the newly developed methods.

Cross-sectioned samples were also imaged using a dual-stain approach to allow for visualization of both cell wall material and lignin (i.e., using Calcofluor White and Acriflavine, respectively) (Figure 32). In Ze-M, a lack of localized Acriflavine fluorescence indicates low levels of lignification as is expected from the maintenance media formulation. In Ze-I samples, grown in induction medium, fluorescent regions of lignification are interspersed throughout the sample. By contrast, the acriflavine fluorescence of the Zinnia stem is localized to the small vascular bundles. These microstructural visualizations indicate that with the present cultivation methods, grown materials present less-ordered growth exhibiting local randomness, but greater macroscopic homogeneity making for improved uniformity of materials overall. Components of tissue which normally occur in small, localized regions within a plant system can achieve larger and more dispersed presentations when grown in gel-mediated cultures.

10.4 Takeaways

- Adjusting media formulation significantly impacts resulting material properties, growth, and microstructure of grown materials.
- Ze-I samples present dense growth with entangled cells and interspersed regions of lignification. Ze-I samples exhibit storage modulus values higher than Ze-M samples.
- Ze-M yields low density materials made up of enlarged, rounded cells with thickened cell walls. As a result of the open microstructure, percent volume increase in Ze-M samples was nearly quadruple the percent mass increase and volume increase for Ze-M samples was roughly four times that of Ze-I samples. Reduced entanglement of cells as a result of their structure is believed to partially explain the reduced storage modulus of Ze-M samples relative to Ze-I samples.
- Grown samples can be made larger and more uniform than naturally occurring tissues. Increased organization and interconnectedness of cellular components would improve the natural likeness of cultured materials and should be explored in future works.
- The growth of these characterized materials was dictated by a single set of applied conditions, but a multi-stage development process may enable useful combinations of cellular traits in materials (i.e., a delayed trigger to differentiate in order to first allow significant growth or elongation).

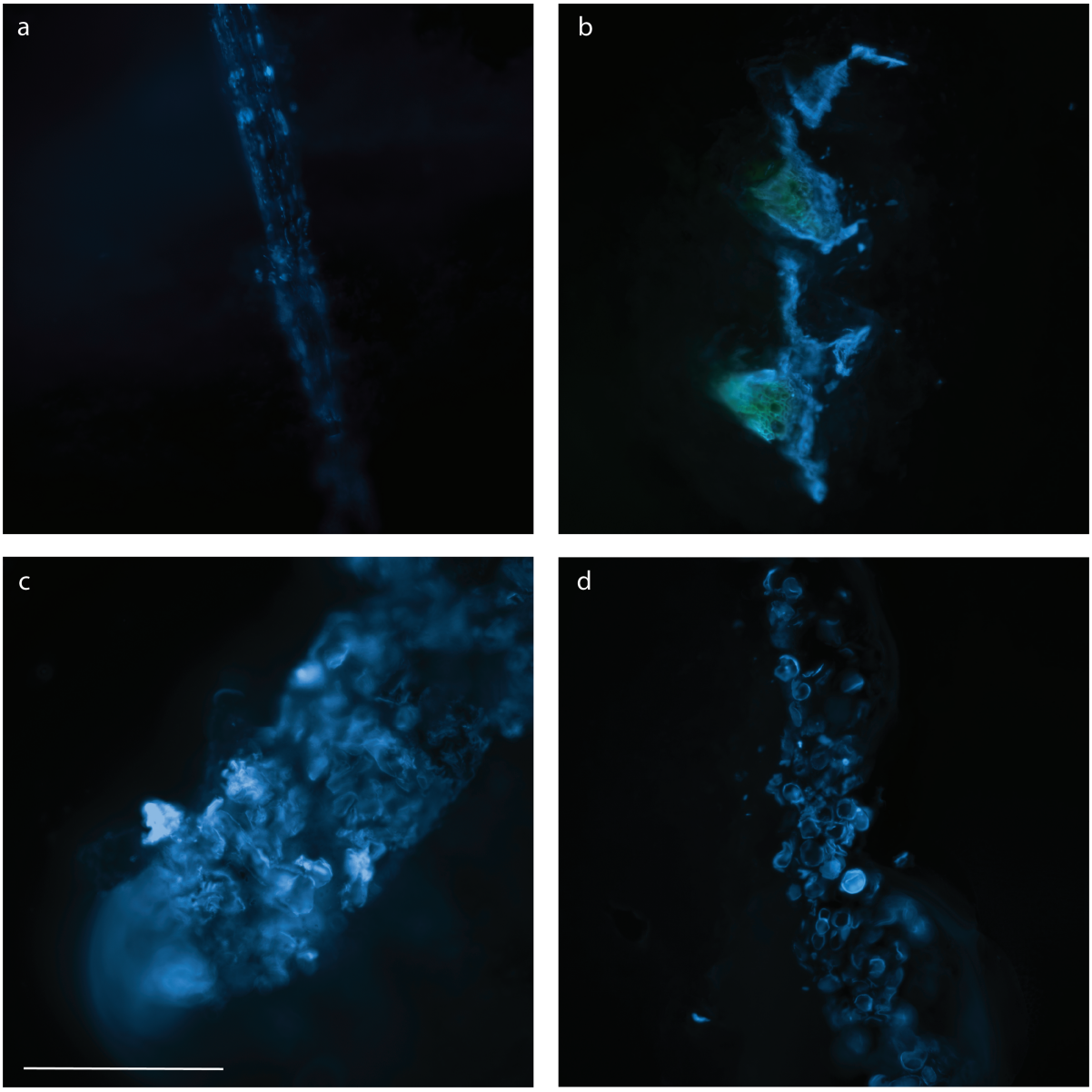

Figure 30: **10x cross-sectional images of various prepared samples and Zinnia stem using CW stain to indicate cell walls.** (a) Growth-free samples exhibit limited and discrete fluorescence where cells have flattened in the dehydration process without convalescing. (b) A halved and dried Zinnia stem, with vascular tissue indicated in green using Acriflavine stain, is delicate, non-homogeneous and small in scale compared to printed samples. (c) Ze-I sample shows dense cell growth. Some elongated cells are visible and cells show good apparent interaction. (d) Ze-M shows open material structure with thick-walled, rounded cells. The cell-to-cell interaction appears to be limited, although some local connectivity may be present. All samples are pictured at the same magnitude. Scale bar equals 500 micrometers.

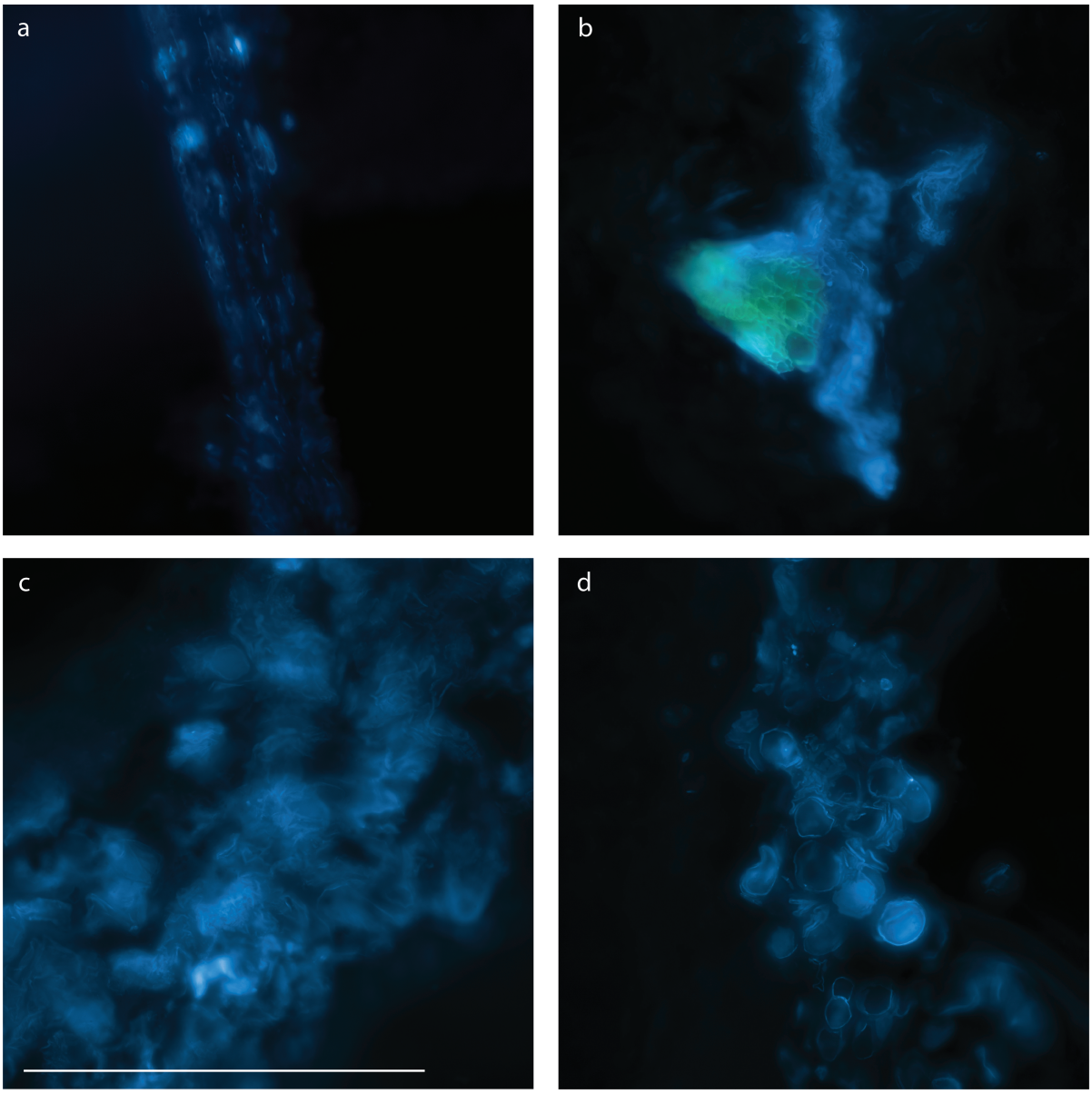

Figure 31: **20x cross-sectional images of various prepared samples and Zinnia stem.** Blue coloration indicates cell walls made visible using CW stain. (a) Growth-free samples exhibit limited and discrete fluorescence where cells have flattened in the dehydration process without convalescing. (b) A Zinnia stem, halved with vascular tissue indicated in green–allowed by staining with Acriflavine, shows tightly-packed cells with lumen of various sizes. (c) Ze-I sample shows dense cell growth and what appear to be frayed secondary cell wall structures of TE's. These structures were likely disturbed during the sectioning process. (d) Ze-M shows open material structure with rounded cells which are well-preserved despite the dehydration process. The cell-to-cell interaction appears to be limited in the Ze-M sample, although some local connectivity may be present. All samples are pictured at the same magnitude. Scale bar equals 500 micrometers.

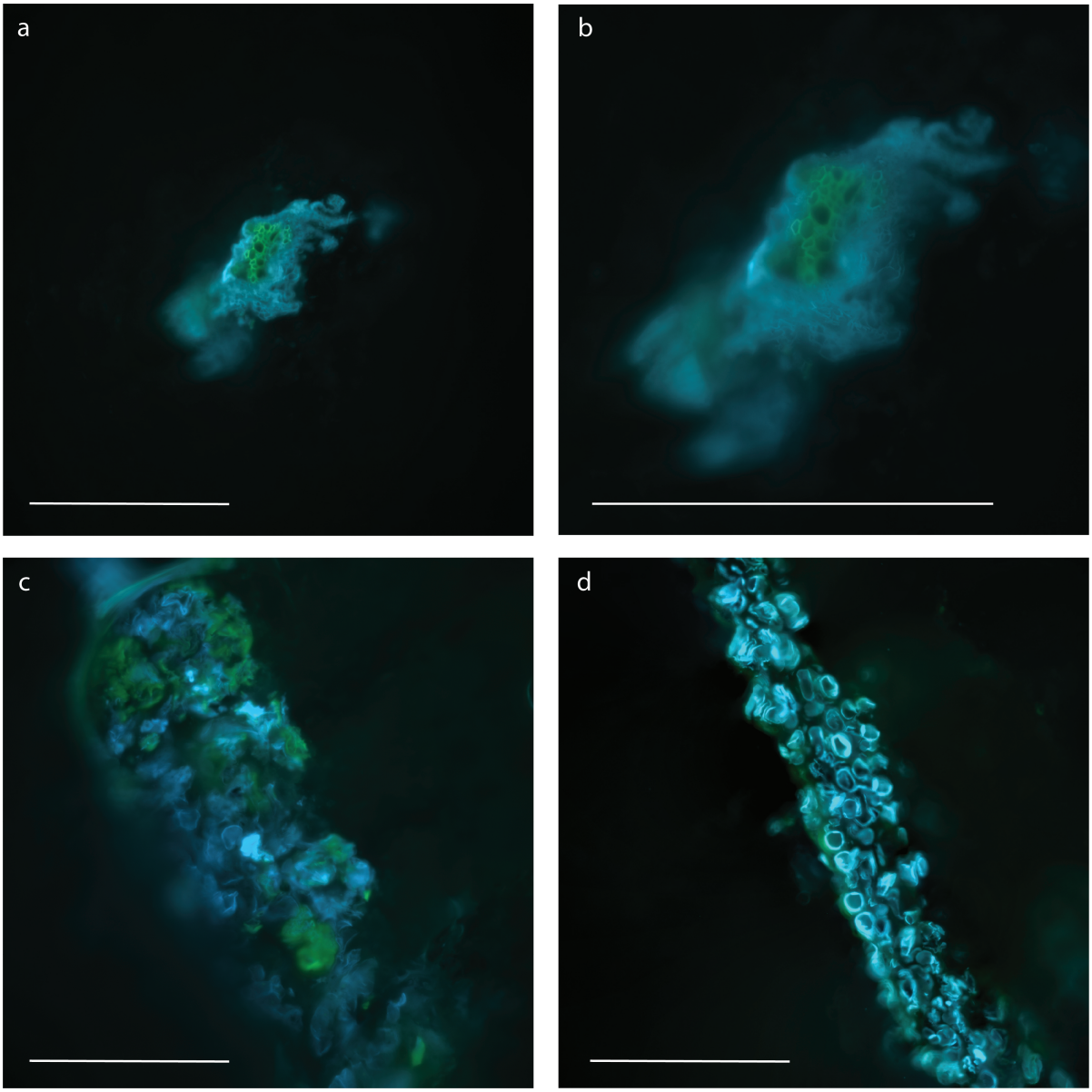

Figure 32: **Dual-stained sample cross-sections allow for cell wall and lignin visualization.** Light blue coloration indicates cell walls, green coloration indicates lignin as stained using Acriflavine. In dried Zinnia stems, imaged at 10x (a) and 20x (b), lignin is localized to a small bundle of vascular tissue. In Ze-I samples (c) Acriflavine fluorescence is dispersed throughout the sample cross-section. In Ze-M samples, there are no obvious regions of specific Acriflavine fluorescence supporting the expected lack of lignified cells. All scale bars represent 500 micrometers.

11 Future Work

Efforts toward the production of *ex vivo* tissue-like plant materials are still in the early stages. The field would benefit from an improved understanding and control of cellular development, advancements to greater synchrony and uniformity of cellular development, a deeper exploration of the relationship between cellular-level characteristics and resulting material properties, and improvements to the consistency and utility of grown materials.

A myriad of factors, known and yet unknown, orchestrate the growth, development, and differentiation of plant cells in both nature and the culture environment. In this work, a few selected, influential factors were examined, and their impact quantified with respect to the four defined metrics. Much remains to be understood about the effects of other chemical (e.g., other hormone, individual ion, and sucrose concentrations, etc.), mechanical (e.g., matrix stiffness, applied loads, etc.), and environmental (e.g., light, temperature, CO2 concentration, electric fields, etc.) cues on cell development in the context of gel-based culture. Beyond these external factors, genetic triggers could be better understood and leveraged to induce the desired development. Improving the predictability, synchrony, and extent of transformation would yield more uniform material results and open the door to more complex cellular instruction. For example, multi-step application of growth cues could ensure the presentation of two traits which do not typically present together (e.g., pronounced elongation and tracheary element differentiation).

Natural mimicry of grown materials could be improved through the induction of cellular alignment. In natural vascular tissues, cells are highly organized and aligned to facilitate fluid flow. In some applications, the natural grain of the material is structurally advantageous or aesthetically desirable. Currently no scalable method exists to direct the alignment of plant cells in a multi-cellular *ex vivo* environment[f]. Furthermore, in the tightly-packed natural structures, cells physically connect to one another through

[f]Zaban *et al.* examine effects of auxin gradients and auxin efflux on single-cell alignment [51]

the middle lamella. This interconnectedness lends strength to the plant material. Ideally culture systems could be made to emulate this interconnectivity. The relationship between the growing cells and the surrounding scaffold also warrants further exploration. Scaffold chemistries could be adjusted to promote cell adhesion or steer cell growth and development. In this way, interfacial interactions between plant and gel phases could be investigated and improved to allow for better mechanical properties.

Both the cellular-level properties (e.g., lignin content of cell walls) and cell-to-cell connectivity are likely to impact the resulting properties of grown materials. Methods should be developed to quantify these relationships in order to inform the production of materials with specific, desired properties. A deeper analysis of the relationships between cell wall properties, cell-matrix interactions, and the results on emergent material properties are needed to be able to better predict material outcomes based on expected culture developments. With further maturation of presented techniques, entirely new plant-based materials could be possible—with spatially controlled microstructures and properties or multi-species materials derived from a monolithically grown culture.

The utility and applicability of these cultivated materials could be improved with process translation and refinement. Translating these techniques to higher-value or higher-utility species would broaden the potential application space and achievable material properties. Optimizing scaffold deposition would allow for improved control over material shape and fabrication of more complex, finer-featured structures. Finally, production scale-up efforts would be aided by an improved understanding of size constraints (e.g., critical culture scales at which growth becomes impaired or behaves unpredictably).

The field of directly cultivated plant materials is still in its infancy. The work encompassed in this thesis provides a first interrogation into the potential of the field and seeks to establish a practical foundation which can inspire future progress in this space.

12 Conclusion

This thesis proposes and explores a biotechnology-driven solution to the burdensome demands on slow-growing plant materials like wood. Such materials typically yield low proportions of high-value plant materials and require energy-intensive harvest and processing to reach a saleable condition. Plant cell culture has the potential to address a number of intrinsic inefficiencies associated with traditional whole-plant cultivation. The newly proposed concept of *net-shape plant material cultivation* allows for localized, high-density, land-free production of net-shape plant materials thereby reducing energy usage associated with harvest, transport, and processing as well as reducing plant waste. Additionally, the presented plant material cultivation methods enable control over emergent physical properties of materials, thus opening the door to a new era of possibilities in the natural materials space (e.g., specialized plant materials with specifically tuned properties or even monolithic plant materials with spatially controlled characteristics).

A *Zinnia elegans* model system was used to provide the first proof-of concept demonstration of isolated, tissue-like plant material production in controlled configurations. In the development and demonstration of these lab-grown plant materials, core efforts were made to understand and tune cell growth, to control material shape to access new forms and scales, and to begin to elucidate relationships between culture conditions and final material outcomes.

In order to direct cell growth in cultures, it was first necessary to understand cell growth. To quantify cell behavior, metrics were developed to evaluate cell development in culture systems. These metrics were then employed to monitor cell response to a range of environmental factors including auxin/cytokinin ratios, pH, initial cell density, and gel culture depth. By simultaneously mapping emergent cellular characteristics in response to a range applied culture conditions, this work demonstrates the potential to guide cellular differentiation and morphologies within gel-based culture systems. The cell response maps, as characterized by the four developed metrics (i.e., live fraction, lignification, enlargement, and elongation metrics) then informed future iterations of

cultured materials to achieve the desired cell-level properties. Across replicated tests, quantified trends in development appeared to be repeatable across biological samples of Zinnia—which speaks to both the utility of the selected metrics and reliability of the Zinnia cell responsiveness to the selected stimuli. Conducted experiments have begun to elucidate relationship between the developed metrics (e.g., the inverse trends between live fraction and differentiation metrics, and elongation and differentiation metrics) enabling the thoughtful direction of culture growth and identifying important areas of future investigation.

With regard to the macroscopic scale, scaffold structure, as controlled by casting or bioprinting, was found to effectively guide plant material growth. Scaffold-guided growth enables the production of plant materials in both forms and at dimensions that are otherwise unavailable using traditional cultivation methods. Although structures in these investigations were kept to planar configurations, cells were also found to be capable of survival when positioned more than 8.7 mm from the gel surface indicating the potential for larger structures to be generated.

Once methods to grow net-shape materials were established, efforts were made to characterize the emergent properties and to understand how changes to culture conditions impacted the mechanical, physical, and microstructural attributes of the systems. Simple adjustments to media formulation were found to significantly impact all three of these characteristics. Samples grown in induction medium (Ze-I) with high levels of auxin and cytokinin presented dense growth with entangled cells and interspersed regions of lignification. Ze-I samples also presented higher storage modulus values than samples grown in low-hormone maintenance medium (at 404.7 MPa $\pm$ 146.9 and 135.3 $\pm$ 57.4 MPa, respectively). Ze-M samples were characterized most notably by low densities and open microstructures. Compared to naturally-occurring plant tissues of the Zinnia, grown samples were much larger and more uniform in that they lack patterned, highly-ordered growth and instead present more locally random, but generally even growth. Increasing organization and interconnectedness of cellular components could improve natural likeness of cultured materials, if desired. Hormone levels also impacted growth

potential in addition to material properties. Samples grown in high hormone media saw only moderate increases in sample volume and mass (91% and 31%, respectively) over the culture period compared to larger gains in low hormone formulations (398% and 119%, respectively) relative to a cell-free control.

In this work, the growth of characterized materials was examined in response to changes to a single applied set of conditions at the outset of culture growth, improved characteristics may be obtainable by making use of a multistage culture wherein developmental are introduced at different time-points (i.e., delay a trigger to differentiate in order to first allow for significant growth or elongation). These opportunities would be worth examining in future investigations.

The concept of tunable, net-shape plant material production is still nascent. This thesis represents a foundational investigation into this research space and indicates the promise of using plant cell culture to selectively generate valuable plant tissues as an alternative to whole-plant cultivation. This work additionally proposes and illustrates novel methods for quantification of cell development and uses the findings to map and direct development by modulating simple input conditions. For materials grown from bioprinted samples, this thesis begins to characterize the complex relationships between cellular-level growth and the emergent material properties. Most importantly, this proof-of-concept illustrates the promise of a new approach to agriculture. With tunable, land-free, net-shape cultivation of plant materials, wood and other plant-based products may one day be obtainable with limited impact to the surrounding natural environment.

References

[1] G F Peter et al. "The value of forest biotechnology: A cost modelling study with loblolly pine and kraft linerboard in the southeastern USA". In: *International Journal of Biotechnology* 9.5 (2007), pp. 415–435. ISSN: 09636048. DOI: 10.1504/IJBT.2007.014269.

[2] M M Campbell et al. "Forestry's fertile crescent: the application of biotechnology to forest trees". In: *Plant Biotechnology Journal* 1.3 (2003), pp. 141–154. DOI: 10.1046/j.1467-7652.2003.00020.x.

[3] T W Crowther et al. "Mapping tree density at a global scale". In: *Nature* 525.7568 (2015), pp. 201–205. ISSN: 14764687. DOI: 10.1038/nature14967.

[4] M C Hansen et al. "High-Resolution Global Maps of". In: 850.November (2013), pp. 850–854. DOI: 10.1126/science.1244693.

[5] M Bologna and G Aquino. "Deforestation and world population sustainability: a quantitative analysis". In: *Scientific Reports* 10.1 (2020), pp. 1–9. ISSN: 20452322. DOI: 10.1038/s41598-020-63657-6. URL: http://dx.doi.org/10.1038/s41598-020-63657-6.

[6] Y P S Bajaj, ed. *Biotechnology in Agriculture and Forestry 5: Trees II*. Berlin: Springer-Verlag, 1989. ISBN: 978-3-642-64862-5. DOI: 10.1007/978-3-642-61535-1.

[7] J Greene. *Pulp & Paper Products Consume 50% of Harvested Timber in US*. URL: https://www.fisheri.com/blog/pulp-paper-products-consume.

[8] T H Stasko et al. "Mapping woody-biomass supply costs using forest inventory and competing industry data". In: *Biomass and Bioenergy* 35.1 (2011), pp. 263–271. ISSN: 09619534. DOI: 10.1016/j.biombioe.2010.08.044. URL: http://dx.doi.org/10.1016/j.biombioe.2010.08.044.

[9] H Rischer, G R Szilvay, and Kirsi Marja Oksman-Caldentey. "Cellular agriculture — industrial biotechnology for food and materials". In: *Current Opinion in Biotechnology* 61 (2020), pp. 128–134. ISSN: 18790429. DOI: 10.1016/j.copbio.2019.12.003.

[10] S Mehrotra et al. "3D Bioprinting in Plant Science: An Interdisciplinary Approach". In: *Trends in Plant Science* 25.1 (2020), pp. 9–13. ISSN: 13601385. DOI: 10.1016/j.tplants.2019.10.014. URL: https://doi.org/10.1016/j.tplants.2019.10.014.

[11] A L Beckwith, J T Borenstein, and L F Velásquez-García. "Tunable plant-based materials via in vitro cell culture using a Zinnia elegans model". In: 288 (2021). DOI: 10.1016/j.jclepro.2020.125571.

[12] A Hussain et al. "Plant Tissue Culture: Current Status and Opportunities". In: *IntechOpen* (2012). DOI: 10.5772/50568.

[13] Y P S Bajaj, ed. *Biotechnology in agriculture and forestry. 17. high-tech and micropropagation I.* Vol. 17. Springer-V, 1991. DOI: 10.1007/978-3-642-76415-8.

[14] H Isikawa. "In vitro culture of forest tree calluses and organs". In: *Jarq* 18.2 (1984), pp. 131–141.

[15] I Y E Chu. *Perspective of Micropropagation Industry.* 1992, pp. 137–150. DOI: 10.1007/978-94-011-2785-1_8.

[16] W Barz, E Reinhard, and M H Zenk, eds. *Plant Tissue Cultuer and Its Biotechnological Application.* Springer-Verlag, 1977, pp. 213–224. DOI: 10.1007/978-3-642-66646-9.

[17] M Ochoa-Villarreal et al. "Plant cell culture strategies for the production of natural products". In: *BMB Reports* 49.3 (2016), pp. 149–158. ISSN: 1976670X. DOI: 10.5483/BMBRep.2016.49.3.264.

[18] M Donini and C Marusic. "Current state-of-the-art in plant-based antibody production systems". In: *Biotechnology Letters* 41.3 (2019), pp. 335–346. ISSN: 15736776. DOI: 10.1007/s10529-019-02651-z.

[19] Y Tekoah et al. "Large-scale production of pharmaceutical proteins in plant cell culture-the protalix experience". In: *Plant Biotechnology Journal* 13.8 (2015), pp. 1199–1208. ISSN: 14677652. DOI: 10.1111/pbi.12428.

[20] R Eibl et al. "Plant cell culture technology in the cosmetics and food industries: current state and future trends". In: *Applied Microbiology and Biotechnology* 102.20 (2018), pp. 8661–8675. ISSN: 14320614. DOI: 10.1007/s00253-018-9279-8.

[21] R Mohammadinejad et al. "Plant molecular farming: Production of metallic nanoparticles and therapeutic proteins using green factories". In: *Green Chemistry* 21.8 (2019), pp. 1845–1865. ISSN: 14639270. DOI: 10.1039/c9gc00335e.

[22] T H Jovic et al. "Plant-Derived Biomaterials: A Review of 3D Bioprinting and Biomedical Applications". In: *Frontiers in Mechanical Engineering* 5.April (2019), pp. 1–18. ISSN: 2297-3079. DOI: 10.3389/fmech.2019.00019.

[23] J Emmermacher et al. "Engineering considerations on extrusion-based bioprinting : interactions of material behavior , mechanical forces and cells in the printing needle Engineering considerations on extrusion-based bioprinting : interactions of material behavior , mechanical f". In: *Biofabrication* 12 (2020). DOI: 10.1088/1758-5090/ab7553.

[24] J Seidel et al. "Green bioprinting: Extrusion-based fabrication of plant cell-laden biopolymer hydrogel scaffolds". In: *Biofabrication* 9.4 (2017). ISSN: 17585090. DOI: 10.1088/1758-5090/aa8854.

[25] R Wightman and C J Luo. "From mammalian tissue engineering to 3D plant cell culture". In: *Biochemist* 38.4 (2016), pp. 32–35. ISSN: 17401194. DOI: 10.1042/bio03804032.

[26] S M Park, H W Kim, and H J Park. "Callus-based 3D printing for food exemplified with carrot tissues and its potential for innovative food production". In: *Journal of Food Engineering* 271 (2020). DOI: 10.1016/j.jfoodeng.2019.109781.

[27] V Vancauwenberghe et al. "3D printing of plant tissue for innovative food manufacturing: Encapsulation of alive plant cells into pectin based bio-ink". In: *Journal of Food Engineering* 263 (2019), pp. 454–464. DOI: 10.1016/j.jfoodeng.2017.12.003.

[28] F Berthiaume, T J Maguire, and M L Yarmush. "Tissue engineering and regenerative medicine: History, progress, and challenges". In: *Annual Review of Chemical and Biomolecular Engineering* 2 (2011), pp. 403–430. ISSN: 19475438. DOI: 10.1146/annurev-chembioeng-061010-114257.

[29] *Apligraf*. URL: https://apligraf.com/.

[30] I Perea-Gil, C Prat-Vidal, and A Bayes-Genis. "In vivo experience with natural scaffolds for myocardial infarction: The times they are a-changin'". In: *Stem Cell Research and Therapy* 6.1 (2015), pp. 1–25. ISSN: 17576512. DOI: 10.1186/s13287-015-0237-4. URL: http://dx.doi.org/10.1186/s13287-015-0237-4.

[31] E Cimetta, A Godier-Furnémont, and G Vunjak-Novakovic. "Bioengineering heart tissue for in vitro testing". In: *Current Opinion in Biotechnology* 24.5 (2013), pp. 926–932. ISSN: 09581669. DOI: 10.1016/j.copbio.2013.07.002.

[32] C Plomion, G Leprovost, and A Stokes. "Wood Formation in Trees". In: *Plant Physiology* 127.December (2001), pp. 1513–1523. ISSN: 00320889. DOI: 10.1104/pp.010816.1.

[33] Y Kondo et al. "Vascular cell induction culture system using arabidopsis leaves (VISUAL) reveals the sequential differentiation of sieve element-like cells". In: *Plant Cell* 28.6 (2016), pp. 1250–1262. ISSN: 1532298X. DOI: 10.1105/tpc.16.00027.

[34] S Turner, P Gallois, and D Brown. "Tracheary Element Differentiation". In: *Annual Review of Plant Biology* 58.1 (2007), pp. 407–433. ISSN: 1543-5008. DOI: 10.1146/annurev.arplant.57.032905.105236.

[35] K H Caffall and D Mohnen. "The structure, function, and biosynthesis of plant cell wall pectic polysaccharides". In: *Carbohydrate Research* 344.14 (2009), pp. 1879–1900. ISSN: 00086215. DOI: 10.1016/j.carres.2009.05.021. URL: http://dx.doi.org/10.1016/j.carres.2009.05.021.

[36] P Twumasi et al. "Establishing in vitro Zinnia elegans cell suspension culture with high tracheary element differentiation". In: *Cell Biology International* 33.4 (2009), pp. 524–533. ISSN: 10656995. DOI: 10.1016/j.cellbi.2009.01.019. URL: http://dx.doi.org/10.1016/j.cellbi.2009.01.019.

[37] A Fehér. "Callus, dedifferentiation, totipotency, somatic embryogenesis: What these terms mean in the era of molecular plant biology?" In: *Frontiers in Plant Science* 10.April (2019), pp. 1–11. ISSN: 1664462X. DOI: 10.3389/fpls.2019.00536.

[38] M Ikeuchi, K Sugimoto, and A Iwase. "Plant callus: Mechanisms of induction and repression". In: *Plant Cell* 25.9 (2013), pp. 3159–3173. ISSN: 10404651. DOI: 10.1105/tpc.113.116053.

[39] Victor M Loyola-Vargas and Felipe Vázquez-Flota, eds. *Plant Cell Culture Protocols*. Second. Totawa: Humana Press, 2006, pp. 4–10. ISBN: 9781493985937. URL: http://www.springer.com/series/7651.

[40] P M Kieran, P F MacLoughlin, and D M Malone. "Plant cell suspension cultures: Some engineering considerations". In: *Journal of Biotechnology* 59.1-2 (1997), pp. 39–52. ISSN: 01681656. DOI: 10.1016/S0168-1656(97)00163-6.

[41] H Fukuda and A Komamine. " Establishment of an Experimental System for the Study of Tracheary Element Differentiation from Single Cells Isolated from the Mesophyll of Zinnia elegans ". In: *Plant Physiology* 65.1 (1980), pp. 57–60. ISSN: 0032-0889. DOI: 10.1104/pp.65.1.57.

[42] C Domingo et al. “A pectate lyase from Zinnia elegans is auxin inducible”. In: *Plant Journal* 13.1 (1998), pp. 17–28. ISSN: 09607412. DOI: 10.1046/j.1365-313X.1998.00002.x.

[43] D Milioni et al. “Early gene expression associated with the commitment and differentiation of a plant tracheary element is revealed by cDNA-amplified fragment length polymorphism analysis”. In: *Plant Cell* 14.11 (2002), pp. 2813–2824. ISSN: 10404651. DOI: 10.1105/tpc.005231.

[44] N R Mustafa et al. “Initiation, growth and cryopreservation of plant cell suspension cultures”. In: *Nature Protocols* 6.6 (2011), pp. 715–742. ISSN: 17542189. DOI: 10.1038/nprot.2010.144.

[45] R Möller et al. “Cell differentiation, secondary cell-wall formation and transformation of callus tissue of Pinus radiata D. Don”. In: *Planta* 217.5 (2003), pp. 736–747. ISSN: 00320935. DOI: 10.1007/s00425-003-1053-0.

[46] B-G Kang et al. “Micropropagation of Populus trichocarpa ’Nisqually-1’: The genotype deriving the Populus reference genome”. In: *Plant Cell, Tissue and Organ Culture* 99.3 (2009), pp. 251–257. ISSN: 01676857. DOI: 10.1007/s11240-009-9596-9.

[47] L Donaldson and N Williams. “Imaging and spectroscopy of natural fluorophores in pine needles”. In: *Plants* 7.1 (2018), pp. 1–16. ISSN: 22237747. DOI: 10.3390/plants7010010.

[48] E Pesquet et al. “Novel Markers of Xylogenesis in Zinnia Are Differentially Regulated by Auxin and Cytokinin”. In: *Plant Physiology* 139.4 (2005), pp. 1821–1839. DOI: 10.1104/pp.105.064337.phloem.

[49] I Ślesak et al. “The role of hydrogen peroxide in regulation of plant metabolism and cellular signalling in response to environmental stresses”. In: *Acta Biochimica Polonica* 54.1 (2007), pp. 39–50. ISSN: 0001527X. DOI: 10.18388/abp.2007_3267.

[50] A Ivakov and S Persson. "Plant cell shape: Modulators and measurements". In: *Frontiers in Plant Science* 4.NOV (2013), pp. 1–13. ISSN: 1664462X. DOI: 10.3389/fpls.2013.00439.

[51] B Zaban et al. "Plant cells use auxin efflux to explore geometry". In: *Scientific Reports* 4 (2014), pp. 1–8. ISSN: 20452322. DOI: 10.1038/srep05852.

[52] L Taiz and E Zeiger. *Plant Physiology*. Toledo: Benjamin-Cummings Publishing Co., 2003. ISBN: 0-8053-0245-X.

[53] H Fukuda. "Tracheary Element Differentiation". In: *The Plant Cell* 9 (1997), pp. 1147–1156. DOI: 10.1105/tpc.9.7.1147.

[54] L Bergmann. "Growth and division of single cells of higher plants in vitro." In: *The Journal of general physiology* 43 (1960), pp. 841–851. ISSN: 00221295. DOI: 10.1085/jgp.43.4.841.

[55] C Schaller. *Polymer Chemistry*. Compiled 2. LibreTexts, 2021. URL: https://chem.libretexts.org/Bookshelves/Organic%7B%5C_%7DChemistry/Book%7B%5C%%7D3A%7B%5C_%7DPolymer%7B%5C_%7DChemistry%7B%5C_%7D(Schaller)/04%7B%5C%%7D3A%7B%5C_%7DPolymer%7B%5C_%7DProperties/4.08%7B%5C%%7D3A%7B%5C_%7DStorage%7B%5C_%7Dand%7B%5C_%7DLoss%7B%5C_%7DModulus.

[56] D Weitz, H Wyss, and R Larsen. "Oscillatory rheology: Measuring the viscoelastic behaviour of soft materials". In: *GIT laboratory journal Europe* 11.3-4 (2007), pp. 68–70. ISSN: 1611-6038. URL: http://cat.inist.fr/?aModele=afficheN%7B%5C&%7Dcpsidt=18678304%7B%5C%%7D5Cnpapers2://publication/uuid/8458E453-11B4-406C-BDC5-101CE8F8D2D8.

[57] A Shrivastava. *Introduction to Plastics Engineering*. William Andrew Publishing, 2018, pp. 49–110. ISBN: 9780323395007. DOI: https://doi.org/10.1016/B978-0-323-39500-7.00003-4.

[58] P Varela, A Salvador, and S Fiszman. "Changes in apple tissue with storage time: Rheological, textural and microstructural analyses". In: *Journal of Food Engineering* 78.2 (2007), pp. 622–629. ISSN: 02608774. DOI: 10.1016/j.jfoodeng.2005.10.034.

[59] PerkinElmer. *Dynamic Mechanical Testing A Beginner's Guide*. 2008. URL: https://www.perkinelmer.com/CMSResources/Images/44-74546GDE%7B%5C_%7DIntroductionToDMA.pdf (visited on 07/05/2021).

[60] D Dunson. "Characterization of Polymers using Dynamic Mechanical Analysis (DMA)". 2017. URL: https://www.eag.com/wp-content/uploads/2017/09/M-022717-Characterization-of-Polymers-using-Dynamic-Mechanical-Analysis.pdf.

[61] A C Backman and K A H Lindberg. "Differences in wood material responses for radial and tangential direction as measured by dynamic mechanical thermal analysis". en. In: *Journal of Materials Science* 36 (2001), pp. 3777–3783. DOI: https://doi.org/10.1023/A:1017986119559.

[62] V Placet, J Passard, and P Perré. "WAVET*, A custom device able to measure viscoelastic properties of wood under water-saturated conditions". en. In: *Maderas. Ciencia y tecnología* 10 (2008), pp. 45–60. DOI: 10.4067/S0718-221X2008000100005.